Luteinizing Hormone Regulates the Phosphorylation and Localization of the Mitochondrial Effector Dynamin Like 1 (DRP1) and Steroidogenesis in the Bovine Corpus Luteum

Michele R. Plewes[2,3], **Xiaoying Hou**[2], **Heather A. Talbott**[2], **Pan Zhang**[2], **Jennifer R. Wood**[4], **Andrea S. Cupp**[4], **John S. Davis**[2,3]

[2]Olson Center for Women's Health, Department of Obstetrics and Gynecology, University of Nebraska Medical Center, 983255 Nebraska Medical Center, Omaha, NE 68198-3255, USA

[3]Veterans Affairs Nebraska Western Iowa Health Care System, 4101 Woolworth Ave, Omaha, NE 68105, USA

[4]Department of Animal Sciences, ANSC A224k, University of Nebraska–Lincoln, Lincoln, NE 68583-0908, USA

Abstract

The corpus luteum is an endocrine gland that synthesizes and secretes progesterone. Luteinizing hormone (LH) activates protein kinase A (PKA) signaling in luteal cells, increasing delivery of substrate to mitochondria for progesterone production. Mitochondria maintain a highly regulated equilibrium between fusion and fission in order to sustain biological function. Dynamin-like-1 (DRP1), is a key mediator of mitochondrial fission. The mechanism by which DRP1 is regulated in the ovary is largely unknown. We hypothesize that LH via PKA differentially regulates the phosphorylation of DRP1 on Ser616 and Ser637 in bovine luteal cells. In primary cultures of steroidogenic small luteal cells, LH and forskolin stimulated phosphorylation of DRP1 (Ser 637) and inhibited phosphorylation of DRP1 (Ser 616). Overexpression of a PKA inhibitor blocked the effects of LH and forskolin on DRP1 phosphorylation. Additionally, LH decreased the association of DRP1 with the mitochondria. Genetic knockdown of the DRP1 mitochondria receptor, and a small molecule inhibitor of DRP1 increased basal and LH-induced progesterone production. Studies with a general Dynamin inhibitor and siRNA knockdown of DRP1 showed that DRP1 is required for optimal LH-induced progesterone biosynthesis. Taken together, the findings place DRP1 as an important target downstream of PKA in steroidogenic luteal cells.

Keywords

Dynamin-like Protein 1; Corpus Luteum; Mitochondria; Steroidogenesis; Progesterone; Bovine; protein kinase A

Introduction

The corpus luteum (CL) is a transient endocrine gland that synthesizes the steroid hormone progesterone, which is essential for the establishment and maintenance of pregnancy in mammals (1). Following ovulation, the granulosa and theca cells of the ovarian follicle differentiate to form the large and small luteal cells, respectively, of the bovine corpus luteum (2). While both cell types produce progesterone, *in vitro* experiments revealed that the large cells produce large quantities of progesterone in the cow, (3, 4), goat (5), and ewe (6). However, when compared to large luteal cells, the small luteal cells are present in much larger numbers and are highly responsive to luteinizing hormone (LH) (7, 8). Luteinizing hormone binds to the LH receptor (LHCGR), a G-protein coupled, transmembrane receptor, present mainly on small luteal cells (9). Canonical signaling by the LHCGR involves stimulation of adenylyl cyclase leading to increases in intracellular cAMP (10), activation of protein kinase A (PKA), phosphorylation of PKA substrates, and ultimately stimulation of steroidogenesis (11–13). Luteal steroid biosynthesis requires energetically active mitochondria for the conversion of cholesterol into progesterone.

Mitochondria are functionally important in cellular physiology and impact cell survival, metabolism, and initiation of cell death mechanisms by producing ATP, free radicals and releasing apoptotic proteins (14, 15). Mitochondria are also structurally dynamic organelles that continuously undergo coordinated fission and fusion forming either individual units or interconnected mitochondrial networks within the cell to sustain biological function and the overall fate of the cell (16). In healthy cells, changes in mitochondrial morphology are under the control of fusion proteins [mitofusin 1 (MFN1), mitofusin 2 (MFN2) and optic atrophy 1 (OPA1)]; and fission proteins [dynamin 1 (DNM1), dynamin 2 (DNM2), dynamin 1-like protein (DNM1L; commonly referred to as DRP1), mitochondrial fission factor (MFF), and fission 1 protein (FIS1)] (15, 17–19). These mitochondrial structural regulators are vital for proper development and tissue function. *In vivo*, *MFN1* or *MFN2* (20) or *OPA1* (21) knockout mice are embryonic lethal, with mice dying at mid-gestation as a result of insufficient mitochondrial fusion. Knockout of genes encoding *DNM2* (22) and *DNM1* (23) are also embryonic lethal in mice; and *DNM1L/DRP1* knockout mice die within two weeks of birth (24). Of the dynamin family, DRP1, a large dynamin GTPase, is a key mediator of outer mitochondrial fission (17). During mitochondrial fission, DRP1 is recruited to the mitochondria where DRP1 binds to its outer mitochondrial receptor, MFF, forming oligomeric complexes that surround to constrict and divide mitochondria. Knockdown of DRP1 and MFF, but not fission protein FIS1, disrupts exogenous stimuli–induced mitochondrial fission and apoptosis (25). Recently, dynamin proteins have become novel targets to treat cardiovascular (26–29) and neurodegenerative diseases (30), as well as, cancer therapy (31).

DRP1 is recognized as the major player in mitochondrial fission in mammals, but the mechanism by which DRP1 is regulated in steroidogenic tissues is largely unknown. DRP1 has a N-terminal GTP binding domain thought to provide mechanical force, a dynamin-like middle assembly domain, a small variable domain, and a C-terminal GTPase effector domain (GED). The GED domain of DRP1 is important for mediating both intra- and

intermolecular interactions that are important for the formation of oligomeric DRP1 complexes and regulation of GTPase activity that control mitochondrial fission (32). Four receptors have been identified that recruit DRP1 to mitochondria: mitochondrial fission 1 protein (FIS1) (33), mitochondrial fission factor (MFF) (34), and mitochondrial dynamics proteins of 49 and 51 kDa (MiD49 and MiD51) (35).

The regulation of DRP1 by post-translational modifications and differential phosphorylation is important for DRP1 translocation to mitochondria and induction of mitochondrial fission. Phosphorylation of DRP1 at Ser616 by protein kinase C (PKC) (36) or cyclin dependent kinase (CDK) 1/Cyclin B (37) results in activation and translocation of DRP1 from cytoplasmic compartment to mitochondrial membrane receptors. Moreover, phosphorylation of DRP1 on Ser616 does not directly affect GTPase activity, but mediates DRP1 interactions with other proteins and mitochondrial receptors to activate fission (38). In contrast, phosphorylation of DRP1 within the GED domain at Ser637 inhibits DRP1 GTPase activity and inhibition of DRP1 translocation to mitochondria, thereby preventing mitochondrial fission (39–41). Further, the inactivation site, Ser637, has a PKA consensus sequence and is widely accepted as a site for phosphorylation by PKA (40). Because LH/PKA signaling and mitochondrial function are central to luteal steroidogenesis, we hypothesize that LH via PKA regulates the phosphorylation of DRP1 Ser637 in bovine luteal cells promoting optimal progesterone biosynthesis. The objectives of the current study were to determine the effects of LH and PKA activation on phosphorylation and localization of DRP1 and determine the contribution of DRP1 and MFF to progesterone secretion in LH-responsive bovine small luteal cells.

Materials and methods

Reagents

Penicillin G-sodium, streptomycin sulfate, HEPES, bovine serum albumin (BSA), deoxyribonuclease l, fetal bovine serum (FBS), Tris-HCl, sodium chloride, ethylenediaminetetraacetic acid (EDTA), ethylene glycol-bis(β-aminoethyl ether)-N,N,N',N'-tetraacetic acid (EGTA), sodium fluoride, $Na_4O_2O_7$, Na_3VO_4, Triton X-100, glycerol, dodecyl sodium sulfate, β-mercaptoethanol, bromophenol blue, Tween-20, paraformaldehyde, Mdivi-1 and phorbol 12-myristate 13-acetate (PMA) were purchased from Sigma-Aldrich (St. Louis, MO, USA). The phosphate buffer solution, DMEM (Calcium-free, 4.0 g/L glucose), Penicillin Streptomycin Solution, trypan blue and Lipofectamine RNAimax were purchased from Invitrogen Corporation (Thermo Fisher, Carlsbad, CA). The opti-MEM, M199 culture medium, and gentamicin sulfate were purchased from Gibco (Thermo Fisher, Waltham, MA, USA). Collagenase was purchased from Atlanta Biologicals (Flowery Branch, GA, USA). No. 1 glass coverslips, microscope slide, and Chemiluminescent substrate (SuperSignal West Femto) were from Thermo Fisher Scientific (Waltham, MA, USA). Fluoromount-G and clear nail polish were purchased from Electron Microscopy Sciences (Hatfield, PA, USA). Bovine LH was purchased from Tucker Endocrine Research Institute (Atlanta, GA) and forskolin was purchased from EMD Millipore (Burlington, MA, USA). Bio-Rad protein assay was purchased from Bio-Rad (Hercules, CA, USA) and the non-fat milk was from local Kroger (Cincinnati, OH, USA).

The siRNA, siGLO, siDNM1L [ON-TARGETplus DNM1L (10059) SMARTpool, 95% matched to bovine) and siMFF (CTM-437194; SMICK-000007; Sense Sequence GUGCUUACGCUGAGUGAAAUU; Anti Sense Sequence UUUCACUCAGCGUAAGCACUU) were purchased from Dharmacon (Lafayette, CO, USA). Enzyme-linked immunosorbent assay kit for progesterone was purchased from DRG International, Inc (Springfield, NJ, USA). Table 1 lists all of the antibodies used in the study.

Tissue collection, cell preparation, and elutriation

Bovine ovaries were collected at a local slaughterhouse from first trimester pregnant cows (fetal crown-rump length < 10 cm). The ovaries were immersed in 70% ethanol and then transported to the laboratory at 4 °C in PBS.

Using sterile technique, the corpus luteum was surgically dissected from the ovary and minced finely using a microtome and surgical scissors. Tissue pieces were dissociated using collagenase (103 U/mL) in basal medium [M199 supplemented with antibiotics (100 U/ml penicillin G-sodium, 100 μg/ml streptomycin sulfate, and 10 μg/ml gentamicin sulfate)] for 45 min in spinner flasks at 37 °C. Following incubation, the supernatant was removed and transferred to a sterile 15 mL culture tube. Cells were then washed three times with sterile PBS, re-suspended in 10 mL of elutriation medium (calcium-free DMEM medium, 4.0 g/L glucose, antibiotics, 25 mM HEPES, 0.1 % BSA, and 0.02 mg/mL deoxyribonuclease l; pH 7.2), and placed on ice. Fresh dissociation medium was added to the remaining undigested tissue and incubated with agitation for an additional 45 min. The remaining cells were collected, washed twice with sterile PBS, and combined with the previous sample. After the final wash, cells were re-suspended in 10 mL of culture medium. Viability of cells was determined using trypan blue and cell concentration was estimated using a hemocytometer prior to cell elutriation.

Freshly dissociated cells were re-suspended in 30 mL elutriation medium. Dispersed luteal cells were enriched for small luteal cells (SLC) via centrifugal elutriation as previously described (42). Cells with a diameter of 15–25 μm were classified as small luteal cells (purity > 90%).

Cell preparation and treatments

Luteal cell cultures were plated in 12-well culture dishes at 5×10^5 cells/well. Cells were cultured in culture media [M199 supplemented with 5% FBS, 0.1% BSA and antibiotics] at 37 °C in an atmosphere of 95% humidified air and 5% CO_2, as described above.

Treatment with LH and forskolin

Prior to treatments, cells were rinsed with PBS and fresh culture medium was placed on cells and equilibrated at 37 °C in atmosphere of 95% air and 5% CO_2 for 2 h. For concentration response experiments, cells were treated with culture medium alone or increasing concentration of LH (0–100 ng/mL) for 0.5 h at 37 °C in atmosphere of 95% air and 5% CO_2. For time-response experiments, cells were treated with culture medium alone, LH (10 ng/mL) or the adenylyl cyclase activator forskolin (10 μM) for 0, 0.5, 1, 4, 6 or 24 h, at 37 °C in atmosphere of 95% air and 5% CO_2.

Drug inhibition of DRP1

To evaluate the role of DRP1 in progesterone synthesis, cells were pre-treated with Mdivi-1 (0, 1, 5, 10, 20, or 50 μM) for 2 h. Following pre-treatment, luteal cells were stimulated with LH (10 ng/mL) for 4 h. Conditioned medium was immediately collected at stored at −20 °C until further analysis.

To further evaluate the role of dynamin proteins on progesterone synthesis, cells were pre-treated with Dynasore (0, 5, 10, 20, 40, or 50 μM) for 2 h. Dynasore is a small molecule GTPase inhibitor that targets DNM1, DNM2 and DNM1L/DRP1. Following pre-treatment, luteal cells were stimulated with LH (10 ng/mL) for 4 h. Conditioned medium was immediately collected at stored at −20 °C until further analysis.

Treatment with adenoviruses

The adenoviruses expressing green fluorescent protein (Ad.GFP), β-galactosidase (Ad.βGal; prepared by Chris Wolford, Ohio State University, Columbus, Ohio) and the endogenous inhibitor of PKA, Ad.PKI were previously described (43–45). In brief, enriched small luteal cells were seeded into 12-well culture dishes and maintained at 37 °C in an atmosphere of 95% humidified air and 5% CO_2 for 24 hours prior to adenoviral infection. The Ad.GFP or Ad.PKI were added to cell cultures in serum-free culture medium. After 2 hours, the media was replaced with M199 enriched with 5% FBS and maintained for an additional 24 h at 37 °C in an atmosphere of 95% humidified air and 5% CO_2. The medium was changed, and cells were equilibrated for 2 h prior to treatment with control medium, LH (10 ng/mL), forskolin (10 μM), or phorbol 12-myristate 13-acetate (PMA; 20 nM) for 4-h. Following treatment, protein was extracted, quantified, and subject to western blotting.

siRNA Knockdown of DNM1L/DRP1 and MFF

DRP1 was knocked down using silencing RNA (siRNA) to determine the effects of DRP1 on progesterone production. In brief, enriched small luteal cell populations were transfected with siGLO, DNM1L/DRP1 siRNA (75 nM) or MFF siRNA (100 nM) for 6 h using Lipofectamine RNAimax in opti-MEM1 culture medium. Following transfection, 5% FBS was added to culture medium and incubations were continued for 48 h. Successful knockdown of DRP1 or MFF was confirmed by western blot for each experiment. Following knockdown of siDNM1L, or siMFF, the medium was changed, and cells equilibrated for 2 h prior to treatment with LH (10 ng/mL) for 4 h. Conditioned medium and cell lysates were immediately collected at stored at −20 °C until further analysis.

Western Blotting Analysis

Following incubation, cells were immediately placed on ice; the medium was removed, and cells rinsed three times with 1 mL of ice-cold PBS. Cells were lysed with 50 μL cell lysis buffer (10 mM Tris, 100 mM NaCl, 1 mM EDTA, 1 mM EGTA, 1 mM NaF, 20 mM $Na_4O_2O_7$, 2 mM Na_3VO_4, 1% Triton X-100, 10% glycerol, 0.1% SDS, and 0.5% deoxycholate containing protease and phosphatase inhibitor cocktail). Cells were removed from the culture dish using a cell scraper and the cell lysates sonicated at 40% power setting (VibraCell, Model CV188) for 3 sec to homogenize the cell lysates. Following sonication, cell lysates were centrifuged at 4 °C at $12,000 \times g$ for 10 min. Protein in the supernatant was

determined by the Bio-Rad protein assay per manufacturer's protocol. Samples were suspended in 6× Laemmli buffer (60 mM Tris-Cl pH 6.8, 2% SDS, 10% glycerol, 5% β-mercaptoethanol, 0.01% bromophenol blue) and placed on a dry heat bath at 100 °C for 6 min.

Proteins (30 μg/sample) were resolved using 10% SDS-PAGE and then transferred to nitrocellulose membranes. Membranes were blocked with TBS-T (10 mM Tris-HCl pH 7.4, 140 mM NaCl, and 0.1% Tween 20) containing 5% non-fat milk solution at room temperature for 1 h. Membranes were incubated in primary antibody (Table 1) for 24 h at 4 °C for detection of total and phosphorylated proteins. Membranes were rinsed three times with TBS-T for 5 min. Membranes were then incubated with appropriate horseradish peroxidase-linked secondary antibody (Table 1) for 1 h at room temperature. Blots were then rinsed three times with TBS-T for 5 min each. Chemiluminescent substrate was applied per manufacturer's instructions. Blots were visualized using a UVP Biospectrum 500 Multi-Spectral imaging system (UVP, Upland, CA, USA) and the percent abundance of immunoreactive protein was determined using densitometry analysis in VisionWorks (UVP).

Total proteins were normalized to ACTB or tubulin prior to calculation of fold induction. The ratio of phosphorylated DRP1 to total DRP1 was determined for each treatment and time point. Fold increases due to treatment (control versus LH, forskolin, or PMA) were then calculated.

Confocal microscopy

For all confocal experiments, sterile No. 1 glass coverslips (22×22 mm) were individually placed in each well of a 6-well culture dish. Enriched small luteal cell cultures were seeded at 5×10^5 cells/well.

The effects of LH or PMA on the phosphorylation of DRP1.—To determine the effects of LH on phosphorylation of DRP1, cells were equilibrated in fresh culture medium enriched with 1% BSA for 2 h prior to treatment with LH (10 ng/mL) or PMA (20 nM). Cells were maintained at 37 °C in an atmosphere of 95% humidified air and 5% CO_2 for 30 min, prior to termination of experiment.

The effects of LH on the colocalization of DRP1 with the mitochondria.—To determine the effects of LH on colocalization of DRP1 with mitochondria, cells were equilibrated in fresh culture medium enriched with 1% BSA for 2 h prior to treatment with control media or LH (10 ng/mL). Cells were maintained at 37 °C in an atmosphere of 95% humidified air and 5% CO_2 for 4 h, prior to termination of experiment.

The effects of MFF on the colocalization of DRP1 with the mitochondria.—To further evaluate the effects of MFF on LH-induced localization of DRP1 with mitochondria, enriched small luteal cell populations were transfected with siGLO, or MFF siRNA (100 nM) for 6 h using Lipofectamine RNAimax in opti-MEM1 culture medium. Following transfection, 5% FBS was added to culture medium and incubations were continued for 48 h. Cells were then equilibrated in fresh culture medium enriched with 1% BSA for 2 h prior

to treatment with control media or LH (10 ng/mL). Cells were maintained at 37 °C in an atmosphere of 95% humidified air and 5% CO_2 for 4 h, prior to termination of experiment.

The effects of Dynasore on LH-induced trafficking of cholesterol from luteal lipid droplets to the mitochondria.—To determine the effects of LH on colocalization of TopFluor Cholesterol with mitochondrial outer membrane protein, TOM20, cells were pre-treated with 5 μM TopFluor Cholesterol (Avanti Polar Lipids) for 48 h to allow incorporation in lipid droplets. Following incubation, cells were washed three times with PBS to remove unincorporated lipid probe from cells. Cells were pre-treated with aminoglutethimide (CYP11A1 inhibitor; 50 μM) for 1 h to prevent cholesterol from exiting the mitochondria as pregnenolone prior to treatment with LH (10 ng/mL) for 6 h. To determine the effects of DRP1 on LH-induced colocalization of TopFluor Cholesterol with TOM20, cells were pre-treated with aminoglutethimide and Dynasore (20 μM) for 1 h prior to treatment with LH. Cells were maintained at 37 °C in an atmosphere of 95% humidified air and 5% CO_2 until termination of experiment.

For all experiments, cells were fixed with 200 μL 4% paraformaldehyde and incubated at 4 °C for 30 min. Cells were rinsed 3 × with 1 mL PBS following fixation and then incubated with 200 μL 0.1% Triton-X in PBS-T (0.1% tween-20) at room temperature for 10 min to permeabilize the membranes. The permeabilized cells were rinsed three times with PBS and then blocked in 5% BSA for 24 h at 4 °C. Cells were then rinsed and appropriate antibodies for co-localization (Table 1) were added to each coverslip and incubated at room temperature for 60 min. Following incubation, cells were rinsed three times with PBS to remove unbound antibody. Cells were then incubated with appropriate secondary antibodies (Table 1) at room temperature for 60 min. Cells were rinsed three times with 1 mL PBS to remove unbound antibody. Following labeling with antibodies, coverslips containing labeled cells were mounted to glass microscope slides using 10 μL Fluoromount-G (Electron Microscopy Sciences). Coverslips were sealed to glass microscope slides using clear nail polish and stored at −20 °C until imaging.

Images were collected using a Zeiss 800 confocal microscope equipped with a 63× oil immersion objective (1.4 N.A) and acquisition image size of 1584 × 1584 pixel (77.96 μm × 77.96 μm), and 1024 × 1024 pixel (101.31 μm × 101.31 μm). The appropriate filters were used to excite each fluorophore and emission of light was collected between 450 to 1000 nm. Cells were randomly selected from each slide and 30–45 z-stacked (0.15 μm) images were generated from bottom to top of each experiment. To determine the effects of LH on Mean fluorescence intensity of phospho-DRP1, Images were converted to maximum intensity projections and processed utilizing ImageJ (National Institutes of Health) analysis software. Mean fluorescence intensity was determined as previously described (46, 47). The JACoP plug-in was used in Image J software to determine the Manders' overlap coefficient for each image as previously described (48) and transformed into percent colocalization by multiplying Manders' overlap coefficient by 100 for all colocalization experiments.

Progesterone Analysis

Progesterone concentrations from conditioned medium was determined using a commercially available enzyme-linked immunosorbent assay (ELISA) kit per manufacturer's protocol. Intra- and inter-assay coefficient of variation was 5.04% and 9.15%, respectively, across 12 assays. Because basal progesterone secretion varies among cell preparations, results were expressed as fold changes. The average progesterone secretion in controls was $1,543 \pm 191$ ng/ml/4 hr, n=29.

Statistical Analysis

Each experiment was performed at least three times each using cell preparations from separate animals and dates of collection. All data are presented as the means $\pm$ SEM. The differences in means were analyzed by one-way ANOVA followed by Tukey's multiple comparison tests to evaluate multiple responses, or by *t*-tests to evaluate paired responses. Two-way ANOVA was used to evaluate repeated measures with Bonferroni posttests to compare means. All statistical analysis was performed using GraphPad Prism software from GraphPad Software, Inc.

Results

Effects of luteinizing hormone (LH) or forskolin on phosphorylation of Dynamin-related protein-1 (DRP1).

Increased phosphorylation of DRP1 leads to opposing regulatory mechanisms of either fission (phospho-Ser616) or fusion (phospho-Ser637) (49). To determine whether DRP1 was differentially phosphorylated in steroidogenic luteal cells, enriched populations of small luteal cells were treated with increasing concentrations of LH (0–100 ng/mL) for 30 min and Western blot was used to determine the phosphorylation of DRP1 (Fig. 1 A). LH stimulated a concentration-dependent increase in the phosphorylation of DRP1 at Ser637 ($P < 0.05$; Fig. 1 B), with maximal increases in phosphorylation at Ser637 observed with 10 ng/mL LH. In contrast, LH provoked a concentration-dependent decrease on the phosphorylation of DRP1 at Ser616 when compared to control treated cells ($P < 0.05$: Fig. 1 C), with maximal reductions in phosphorylation at Ser616 observed with 10 ng/mL LH

To determine the temporal nature of the differential phosphorylation of DRP1, small luteal cells were treated with LH (10 ng/mL) or the adenylyl cyclase activator forskolin (10 μM) for up to 24 h and Western blot was used to determine the phosphorylation of DRP1 (Fig. 2 A). Under these conditions LH-induced progesterone accumulation reached maximal levels after 4-h (Fig. 2 B). Treatment with LH stimulated a 2.6-fold increase in the phosphorylation of DRP1 (Ser637) within 30 min when compared to control (0-h; $P < 0.05$; Fig. 2 C). The phosphorylation of DRP1 (Ser637) was maximal after 1-h and remained elevated throughout the experimental period albeit at a lower level and approached control levels after 24 h. Treatment with LH also caused a rapid and significant decrease in the phosphorylation of DRP1 (Ser616) within 30 min (60% decrease; $P < 0.05$; Fig. 2 D). The phosphorylation of DRP1 (Ser616) was reduced throughout the experimental period; yet, approached control after 24 h.

Treatment with the adenylyl cyclase activator forskolin exerted responses similar to those observed in response to LH. Forskolin increased phosphorylation of DRP1 (Ser637) within 30 min (2.5-fold; P < 0.05; Fig. 2 E). The stimulatory response to forskolin was further increased after 1 h (3.2-fold) and slowly diminished toward controls over 24 h of incubation. Treating cells with forskolin also significantly decreased the phosphorylation of DRP1 (Ser616) within 30 min when compared controls (50% decrease, P < 0.05; Fig. 2 F). The phosphorylation of DRP1 (Ser616) was reduced throughout the experimental period; however, approached control at later time points.

DRP1 is regulated by differential phosphorylation events, which are directly mediated by PKA (Ser637) and/or PKC/ERK (Ser616) signaling. We employed confocal microscopy to further determine the effect of LH/PKA on phosphorylation of DRP1. Representative micrographs showing the phosphorylation of DRP1 in response to LH and PMA, an activator of PKC/ERK signaling in luteal cells (50), are shown in Figure 3. Treatment with LH increased the mean fluorescent intensity of phospho-DRP1 on Ser637 193% when compared to control treated cells (P < 0.05; Fig. 3 B). Treatment with PMA also resulted in a modest increase in the mean fluorescent intensity of phospho-DRP1 on Ser637 when compared to control treated cells (P < 0.05; Fig. 3 B). In contrast, LH reduced the mean fluorescent intensity of phospho-DRP1 on Ser616 (P < 0.05; Fig. 3 C); while treatment with PMA increased in the mean fluorescent intensity of phospho-DRP1 on Ser616 153% when compared to control treated cells (P < 0.05; Fig. 3 C).

Effects of inhibition of Protein Kinase A on phosphorylation of DRP1.

To determine the role of PKA activation on the phosphorylation of DRP1, we employed a replication-deficient adenovirus containing the complete sequence of the endogenous inhibitor of PKA (PKI; Ad.PKI) (45). A representative Western blot showing the requirement for PKA on the responses to LH and forskolin is shown in Figure 4. Treatment with Ad.PKI abrogated the stimulatory effects of treatment with LH or forskolin on the phosphorylation of DRP1 on Ser637 when compared to control or Ad.GFP-infected cells (P < 0.05; Fig. 4 B). Treatment with Ad.PKI also completely blocked the ability of LH or forskolin to reduce the phosphorylation of DRP1 on Ser616 when compared to control or Ad.GFP-infected cells P > 0.05; Fig. 4 C). As expected, the stimulatory effects of LH on progesterone were blocked 73% by treatment with Ad.PKI (data not shown).

In contrast to PKA signaling, activation of PKC/ERK signaling has been shown to stimulate phosphorylation of DRP1 on the Ser616 residue (51). To test whether PKA and PKC signaling differentially regulated phosphorylation of DRP1 at Ser616, we treated luteal cells with PMA, a protein kinase C activator previously shown to increase ERK MAPK signaling in bovine luteal cells (50, 52). Treatment with PMA stimulated a robust 4.5±0.4-fold increase (P < 0.05, n = 3) in phosphorylation of DRP1 on Ser616 and a modest increase in phosphorylation of DRP1 on Ser637 (1.9 ± 0.6-fold increase) (Fig. 4 A).

Treatment with Ad.PKI did not alter phosphorylation of DRP1 on Ser637 in cells treated with PMA when compared to Ad.GFP-infected cells (PMA, 1.9 ± 0.6 vs Ad.PKI+PMA, 2.2±0.3; P > 0.05; Fig. 4 A). Treatment with Ad.PKI did not significantly reduce the

stimulatory effect of PMA on the phosphorylation of DRP1 (Ser616) (PMA, 4.5±0.4 vs Ad.PKI+PMA, 3.2±0.6; P > 0.05, n = 3; Fig. 4 A).

Effects of LH on colocalization of DRP1 with mitochondria.

Studies have shown that DRP1 translocates from the cytosol to the mitochondria to interact and mediate mitochondria fission (53). In the present study, confocal microscopy was used to determine the influence of LH and PKA on the co-localization of DRP1 with mitochondria (Fig. 5). In control cells, under basal conditions 62.6±3.0% (mean ± sem) of the immunoreactive DRP1 was colocalized with the mitochondria (Fig. 5, A and B). Following treatment with LH for 4 h there was a 46% decrease in co-localization of DRP1 with the mitochondria (P < 0.05; Fig. 5 B).

In cells transfected with Ad.βGal, under basal conditions 62.6±2.7% (mean ± sem) of the immunoreactive DRP1 was colocalized with the mitochondria (Fig. 5, A and B). Following treatment with LH for 4 h there was a 52% decrease in co-localization of DRP1 with the mitochondria (P < 0.05; Fig. 5 B). In cells transfected with Ad.PKI, under basal conditions 60.6±1.4% (mean ± sem) of the immunoreactive DRP1 was colocalized with the mitochondria (Fig. 5, A and B). Surprisingly, blocking PKA did not elevate DRP1 association with the mitochondria under basal conditions compared to control and Ad.βGal transfected cells (Fig. 5 B). Additionally, in cells transfected with Ad.PKI, treatment with LH was able to promote only a slight decrease in co-localization of DRP1 with Mitotracker (14%), which did not different from control cells transfected with Ad.PKI (P > 0.05; Fig. 5 B).

Effect of the selective DRP1 inhibitor, Mdivi-1, on progesterone production.

To determine the role of DRP1 on LH-induced progesterone secretion enriched populations of small luteal cells were treated with increasing concentrations of Mdivi-1, a small molecule inhibitor specific for DRP1 (54). We observed a biphasic effect of Mdivi-1 on progesterone secretion. Treatment with 1, 5, and 10 μM Mdivi-1 increased basal progesterone secretion (P < 0.05; Fig. 6) and 50 μM Mdivi-1 decreased basal progesterone (P < 0.05; Fig. 6). Likewise, treatment with 1 and 5 μM Mdivi-1 increased LH-induced progesterone secretion (P < 0.05; Fig. 6) and treatment with 50 μM Mdivi-1 decreased LH-induced progesterone (P < 0.05; Fig. 6).

Knockdown of Mitochondrial Fission Factor (MFF) increases progesterone production in small bovine luteal cells.

We demonstrated that LH/PKA-induced inactivation of DRP1 (phosphorylation of DRP1 at Ser637) and inhibition of DRP1 with Mdivi-1 promotes progesterone production. Since both phosphorylation of DRP1 at Ser637 and inhibition of DRP1 using Mdivi-1 prevent localization and interaction of DRP1 with MFF, the mitochondrial membrane receptor for DRP1, we employed specific siRNA targeting MFF to evaluate the role of DRP1 in small luteal cells (Fig. 7). Western blotting revealed a 75% decrease in expression of MFF in siMFF-treated luteal cells when compared to control cells (P < 0.05; Fig. 7 A). Treatment of luteal cells with siMFF resulted in a 40% increase in basal progesterone secretion (P < 0.05;

Fig. 7 B). Treatment of luteal cells with siMFF also resulted in a modest increase in LH-induced progesterone secretion when compared to control cells, ($P < 0.05$; Fig. 7 B).

In siCTL treated cells, under basal conditions $44.6 \pm 1.9\%$ (mean $\pm$ sem) of the immunoreactive DRP1 was colocalized with the mitochondrial marker, Mitotracker (Fig. 7, C and D). In cells treated with siCTL, following treatment with LH for 4 h there was a significant decrease in co-localization of DRP1 with the mitochondria (34.6%, $P < 0.05$; Fig. 7 D), and a corresponding decrease in co-localization of DRP1 with its mitochondrial receptor MFF (31.8%, $P < 0.05$; Fig. 7 E). Compared to siCTL cells approximately 50% less immunoreactive DRP1 was colocalized with the mitochondria (Fig. 7, C and D) or MFF (Fig. 7, C and E) in siMFF knockdown cells, under basal conditions ($P < 0.05$, mean $\pm$ sem). These findings indicate knockdown of MFF effectively reduced DRP1 binding to luteal mitochondria. Additionally, in cells transfected with siMFF, treatment with LH was no longer able to promote decreases in co-localization of DRP1 with either mitochondria (Fig. 7, C and D) or MFF (Fig. 7, C and E).

Knockdown of Dynamin 1-like (DNM1L/DRP1) inhibits progesterone production in small bovine luteal cells.

Another approach to determine the role of DRP1 employed specific siRNA targeting DRP1. Western blotting revealed a 68% decrease in expression of DRP1 in siDNM1L-treated luteal cells when compared to control cells ($P < 0.05$; Fig. 8, A and B). Stimulation with LH had no influence on expression of DRP1 in both siCTL and siDNM1L treated cells ($P > 0.05$; Fig. 7 B). Treatment of luteal cells with siDNM1L resulted in a 49.3% reduction in basal progesterone secretion ($P < 0.05$; Fig. 8 D). Treatment of luteal cells with siDNM1L also resulted in a 50% decrease in LH-induced progesterone secretion when compared to control cells, ($P < 0.05$; Fig. 8 D). The decrease in progesterone was not a result of a reduction in levels of components required for progesterone synthesis (Fig. 8 A). Stimulation with LH lead to a 227% and 241% increase in STAR protein expression in siCTL- and siDNM1L-treated cells, respectively, when compared to control ($P < 0.05$; Fig. 7 D). LH provoked a 35% and 33% increase in CYP11A1 in cells treated with siCTL and siDNM1L, respectively; however, this difference was not significantly different between siRNA treatments ($P > 0.05$). Likewise, stimulation with LH lead to a 22% and 19% increase in HSD3B expression for siCTL and siDNM1L, respectively; which was not significantly different between siRNA treatments ($P > 0.05$).

Dynamin family inhibitor, Dynasore, decreased LH-induced progesterone production and colocalization of TopFluor Cholesterol with mitochondria in small luteal cells.

Although not extensively studied, reports indicate that dynamin-family regulation and mitochondrial homeostasis is important in reproductive tissues (55, 56). Moreover, DNM2, a dynamin-family protein has been suggested to play a role in mitochondrial fission, although this remains controversial. To provide additional evidence for a role of Dynamins on LH-induced progesterone secretion, small luteal cells were treated with increasing concentrations of the dynamin inhibitor Dynasore, a small molecule GTPase inhibitor that targets DNM1, DNM2 and DNM1L/DRP1 (57). Treatment with Dynasore did not alter basal progesterone secretion ($P > 0.05$; Fig. S1 A) However, Dynasore caused a concentration-

dependent reduction in LH-induced progesterone secretion, evident only at relatively high concentrations ($P < 0.05$; Fig. S1 A). Importantly, Dynasore had no influence on LH-induced phosphorylation of DRP1 at Ser637, indicating a potential indirect mechanism for attenuating LH-induced progesterone production ($P > 0.05$; Fig. S1 B).

An emerging role of DNM2 is the regulation of cellular cholesterol, and Dynasore has been reported to impact intracellular cholesterol homeostasis (58, 59). The rate-limiting step to steroidogenesis in the corpus luteum is cholesterol availability and transporting free cholesterol across the mitochondria. In addition to targeting dynamin proteins DNM1, DNM2 and DRP1, Dynasore also blocks dynamin-dependent endocytosis, a mechanism used to in import lipoproteins from the blood for progesterone production. Confocal microscopy was used to determine whether Dynasore influenced mobilization of cholesterol to the mitochondria (Fig. S1 C). To determine the effects of Dynasore on LH-induced cholesterol mobilization from lipid droplets to mitochondrial enriched populations of small luteal cells were pre-loaded with TopFluor Cholesterol for 48 h to allow incorporation in lipid droplets. Cells were pre-treated with aminoglutethimide to inhibit CYP11A1, preventing cholesterol from exiting the mitochondria as pregnenolone, and allowing accumulation of TopFluor Cholesterol within the mitochondria. We observed a significant 2-fold increase in the percent colocalization of TopFluor Cholesterol with the mitochondrial marker TOM20 following LH stimulation in control cells ($P < 0.05$; Fig. S1, C–E). To determine the influence of Dynasore on LH-induced trafficking of TopFluor cholesterol from lipid droplets to mitochondria, we pretreated cells with Dynasore (20 μM) for 1-h prior to stimulation with LH. There was no change in the percent colocalization of TOM20 with TopFluor Cholesterol following LH stimulation for cells treated with Dynasore ($P > 0.05$; Fig. S1, D, F and G), indicating that Dynasore treatment disrupted cholesterol homeostasis in LH-stimulated luteal cells corresponding to a disruption in progesterone synthesis.

Discussion

The function of DRP1 has been extensively studied; however, the mechanism by which DRP1 is regulated in ovarian tissues is largely unknown. The dynamic regulation of mitochondrial fusion and fission on mitochondrial morphology and cell fate has been studied in many physiologic systems, however little work regarding steroidogenesis has been conducted, specifically within the corpus luteum. To our knowledge, the present study provides the first demonstration that LH via a PKA signaling pathway regulates the phosphorylation and localization of DRP1 within mitochondria of the steroidogenic cells of the ovary. We observed that LH and PKA activators differentially phosphorylate DRP1 on residues known to reduce its activity and association with mitochondria. Approaches using a selective small molecule inhibitor of DRP1 and genetic disruption of MFF, the mitochondrial DRP1 receptor, resulted in elevated luteal progesterone production. Our findings indicate that DRP1 is a LH and PKA sensitive molecule that modulates steroidogenesis in the corpus luteum.

LH and PKA signaling are central for luteal steroidogenesis. Using LH-responsive small luteal cells, we found that LH and forskolin differentially regulate the phosphorylation of DRP1 at specific sites known to either inhibit or activate DRP1. LH and forskolin rapidly

stimulated the phosphorylation of DRP1 Ser637, an event associated with inactivation of DRP1 (40). Temporal studies revealed that the increases in DRP1 Ser637 phosphorylation were rapid and sustained for over 6 h following treatment with LH and forskolin. Moreover, the responses to LH and forskolin were associated with a rapid loss of phosphorylation on Ser616 in the DRP1 activation domain. The reductions in phosphorylation at the Ser616 site failed to completely rebound to basal levels throughout the 24 h duration. The pronounced increases in phosphorylation on DRP1 Ser637 and reduction on DRP1 Ser616 suggest that LH inactivates DRP1; in fact, the ratio of Ser637/Ser616 phosphorylation observed under basal conditions increased over six-fold following treatment with LH or forskolin. The LH-induced changes in DRP1 phosphorylation (i.e., inactivation of DRP1) were accompanied by a 42% reduction in DRP1 localized on luteal mitochondria, reducing the ability of DRP1 to remodel luteal mitochondria. Thus, the rapid reduction in the ability of DRP1 to associate with and act on the mitochondria accompanies a rapid increase in luteal progesterone following LH treatment.

The ability of LH and PKA to control DRP1 phosphorylation presumptively inhibits DRP1 activity. Active DRP1 is recruited to potential fission sites at the surface of the mitochondria (60) and the energy generated from GTP hydrolysis provides the mechanical force needed for mitochondrial fission (61). Unlike other Dynamins within the Dynamin family of proteins, DRP1 has evolved to form structures that fit the dimensions of the mitochondria (61). However, PKA-dependent phosphorylation of DRP1 at Ser637 blocks GTPase activity (40). We investigated the role of PKA signaling on DRP1 phosphorylation by utilizing a replication-deficient adenovirus that expresses the endogenous inhibitor of PKA, PKI. Overexpression of PKI abrogated both LH- and forskolin-induced phosphorylation of DRP1 on Ser637, demonstrating that LH-induced phosphorylation of DRP1 at Ser637 is regulated by PKA in small luteal cells. Blocking PKA activity also reversed the inhibitory effect of LH and forskolin on the phosphorylation of DRP1 on Ser616, a site associated with DRP1 recruitment to the mitochondria. The exact mechanism by which LH via PKA reduces phosphorylation of DRP1 Ser616 is unclear but could involve the direct phosphorylation and activation of a phosphoprotein phosphatase. Such a mechanism has been reported in rat granulosa cells in which PKA activates Protein Phosphatase 1 (PP1) and stimulates the dephosphorylation of serine residues on key regulatory molecules (62, 63). Additionally, a similar mechanism was reported in Leydig cells, linking cyclin dependent kinase 1 (CDK1) as a regulator of the phosphorylation of DRP1 at Ser616 (56). Intracellular cAMP signaling decreases CDK1 activity and therefore may not only increase DRP1 Ser637 phosphorylation, but also can decrease DRP1 Ser616 phosphorylation. We tested this possibility in our laboratory; however, we determined that terminally differentiated bovine steroidogenic luteal cells used in our studies do not express CDK1, and an inhibitor of CDK1 had no effect (not shown). Although DRP1 phosphorylation at Ser616 is not directly correlated to the recruitment of DRP1 to mitochondria (49) recruitment to mitochondria is regulated by the phosphorylation status of the DRP1 receptor, MFF. The energy-sensing adenosine monophosphate (AMP)-activated protein kinase (AMPK) directly phosphorylates MFF and is sufficient to rapidly promote mitochondrial fragmentation in mouse embryonic fibroblasts (64). Since LH and PKA inhibit AMPK activity in luteal cells (65), it seems likely that LH-induced inhibition of AMPK disrupts the binding of DRP1 to mitochondria in

luteal cells. The ability of LH, via active PKA signaling, to coordinately regulate both DRP1 and AMPK activity would ensure a reduction both in enzyme activity and localization to mitochondria.

The findings in this study indicate that hormonal regulation of DRP1 is required for optimal progesterone synthesis by luteal cells. This conclusion is supported by approaches using small molecule inhibitors and siRNA mediated knockdown of key molecules. Treatment with Mdivi-1, a compound widely reported to inhibit DRP1-dependent fission, increased basal and LH-stimulated progesterone in a concentration dependent manner. However, Mdivi-1 has been reported to reversibly inhibit complex I and modify mitochondrial ROS production (66), which may influence steroidogenesis independent of DRP1. Therefore, we selected a silencing RNA targeted for the DRP1 receptor, MFF, to inhibit the translocation of active DRP1 to the mitochondria without disrupting mitochondrial respiration and labile cholesterol as seen with other DRP1 chemical inhibitors (58, 59). We observed a 48.7% reduction in the localization of DRP1 with the mitochondria and a significant increase in both basal and LH-induced progesterone biosynthesis. In contrast, knock-down of DRP1 with RNA interference gene targeting reduced levels of DRP1 and partially inhibited LH-stimulated progesterone production. The knockdown of DRP1 did not alter the expression of steroidogenic proteins, STAR, CYP11A1, and HSDB3 indicating that the steps leading to conversion of cholesterol to progesterone were intact. Thus, mitochondrial remodeling may play an important role in cholesterol trafficking for progesterone synthesis. We also observed that the general Dynamin inhibitor Dynasore disrupted progesterone synthesis in LH-stimulated luteal cells. The inhibitory effect of Dynasore involved a blockage of cholesterol trafficking from lipid droplets to mitochondria, a response consistent with known actions of Dynasore on endocytosis and intracellular trafficking of vesicles (58, 59). Collectively, these findings suggest that DRP1 is important for luteal steroidogenesis, although further studies are required to determine how DRP1 localization facilitates LH-induced progesterone production and how downregulation of DRP1 leads to decreased progesterone biosynthesis.

It is well-documented that DRP1-mediates mitochondrial fragmentation associated with apoptotic events in numerous cell types (31, 67–70). It is intriguing to speculate that DRP1 may mediate events involved regression of the corpus luteum. In the bovine, prostaglandin (PG) F2α is the luteolysin that acts on luteal cells, leading to inhibition of progesterone biosynthesis and induction of apoptosis within the corpus luteum (71). The proximal signaling pathway activated following binding of PGF2α to its receptor is the phosphatidylinositol-phospholipase C intracellular signaling pathway that leads to activation of PKC and expression of genes that result in induction of apoptosis within the corpus luteum (71). Here we show that PMA, a PKC activator, stimulates a robust phosphorylation of DRP1 at Ser616, and this phosphorylation is independent of PKA activation. A recent study shows that the extracellular signal-regulated kinase (ERK) mitogen-activated protein kinase (MAPK) ERK2 leads to Ser616 phosphorylation and activation of DRP1 leading to mitochondrial fragmentation in mammalian cancer cells (51). Treatment of large luteal cells with either PGF2α or PMA leads to activation of ERK signaling via PKC (52), and ultimately apoptosis (72–74). Furthermore, PGF2α actives AMPK in bovine large luteal cells (75), which could recruit DRP1 to mitochondria. Caution is needed with this

speculation because studies have demonstrated opposing effects of AMPK on DRP1, both inhibiting (76–80) and promoting DRP1-mediated mitochondrial fission (64). Additional experiments are needed to determine whether DRP1 plays a role in PGF2α-induced luteal regression.

In conclusion, the present study indicates that stimulation of luteal cells with LH regulates the phosphorylation and inhibits the mitochondrial localization of DRP1, and this ability requires the activation of PKA in luteal cells. Genetic knockdown of the DRP1 mitochondria receptor, mitochondria fission factor (MFF) and a small molecule inhibitor of DRP1 Mdivi-1, increased basal and LH-induced progesterone production. These findings imply that LH may stabilize luteal mitochondria and promote cholesterol trafficking for steroidogenesis in bovine luteal cells via modulating the phosphorylation and activity of the mitochondrial fission protein DRP1. These findings place DRP1 as an important target downstream of PKA in ovarian steroidogenic cells.

Supplementary Material

Refer to Web version on PubMed Central for supplementary material.

Acknowledgment

Abbreviations

ACTB	Beta Actin
ANOVA	analysis of variance
BSA	Bovine serum albumin
CDK	cyclin dependent kinase
CL	corpus luteum
CYP11A1	cholesterol side-chain cleavage enzyme, mitochondrial
DNM1	dynamin 1
DNM2	dynamin 2
DRP1	Mitochondrial Effector Dynamin Like 1
ERK1/2	extracellular signal-regulated protein kinase

FBS	Fetal bovine serum
FIS1	fission 1 protein
GED	GTPase effector domain
GFP	green fluorescent protein
HSD3B	3 beta-hydroxysteroid dehydrogenase/Delta 5→4 isomerase type 1
LH	luteinizing hormone
LHCGR	Luteinizing hormone receptor
MFF	mitochondrial fission factor
MFN1	mitofusin 1
MFN2	mitofusin 2
MiD49/51	mitochondrial dynamics proteins of 49 and 51 kDa
OPA1	optic atrophy 1
PKA	protein kinase A
PKC	protein kinase C
PMA	phorbol 12-myristate 13-acetate
SEM	standard error of the mean
SLC	small luteal cell
STAR	steroidogenic acute regulatory protein

References

1. Johnson KR, and Erb RE (1962) Maintenance of pregnancy in ovariectomized cattle with progestin compounds and their effect on progestin levels in the corpus luteum. J Dairy Sci 45, 633–639

2. Donaldson L, and Hansel W (1965) Histological study of bovine corpora lutea1. J Dairy Sci 48, 905–909 [PubMed: 14330748]

3. Alila HW, Dowd JP, Corradino RA, Harris WV, and Hansel W (1988) Control of progesterone production in small and large bovine luteal cells separated by flow cytometry. J Reprod Fertil 82, 645–655 [PubMed: 3163003]

4. Hansel W, Alila HW, Dowd JP, and Yang XZ (1987) Control of steroidogenesis in small and large bovine luteal cells. Aust J Biol Sci 40, 331–347 [PubMed: 3327492]

5. Arikan , Kalender H, and Simsek O (2010) Effects of cholesterol on progesterone production by goat luteal cell subpopulations at two different stages of the luteal phase. Reprod Domest Anim 45

6. Harrison L, Kenny N, and Niswender G (1987) Progesterone production, LH receptors, and oxytocin secretion by ovine luteal cell types on days 6, 10 and 15 of the oestrous cycle and day 25 of pregnancy. J Reprod Fertil 79, 539–548 [PubMed: 3572885]

7. Wiltbank M, Diskin M, and Niswender G (1991) Differential actions of second messenger systems in the corpus luteum. J Reprod Fertil. Supplement 43, 65–75

8. Hansel W, Alila HW, Dowd JP, and Milvae RA (1991) Differential origin and control mechanisms in small and large bovine luteal cells. J Reprod Fertil Suppl 43, 77–89 [PubMed: 1843353]

9. Takao Y, Honda T, Ueda M, Hattori N, Yamada S, Maeda M, Fujiwara H, Mori T, and Wimalasena J (1997) Immunohistochemical localization of the LH/HCG receptor in human ovary: HCG enhances cell surface expression of LH/HCG receptor on luteinizing granulosa cells in vitro. Mol Human Reprod 3, 569–578

10. Marsh JM (1976) The role of cyclic AMP in gonadal steroidogenesis. Biol Reprod 14, 30–53 [PubMed: 177107]

11. Davis J, Weakland L, Farese R, and West L (1987) Luteinizing hormone increases inositol trisphosphate and cytosolic free Ca2+ in isolated bovine luteal cells. J Biol Chem 262, 8515–8521 [PubMed: 3496333]

12. Miller WL (2017) Disorders in the initial steps of steroid hormone synthesis. J Steroid Biochem Mol Biol 165, 18–37 [PubMed: 26960203]

13. Ascoli M, Fanelli F, and Segaloff DL (2002) The lutropin/choriogonadotropin receptor, a 2002 perspective. Endocrine Rev 23, 141–174 [PubMed: 11943741]

14. McBride HM, Neuspiel M, and Wasiak S (2006) Mitochondria: more than just a powerhouse. Curr Biol : CB 16, R551–560 [PubMed: 16860735]

15. Westermann B (2010) Mitochondrial fusion and fission in cell life and death. Nature Rev Mol Cell Biol 11, 872 [PubMed: 21102612]

16. Scott I, and Youle RJ (2010) Mitochondrial fission and fusion. Essays Biochem 47, 85–98 [PubMed: 20533902]

17. Roy M, Reddy PH, Iijima M, and Sesaki H (2015) Mitochondrial division and fusion in metabolism. Curr Opinion Cell Biol 33, 111–118 [PubMed: 25703628]

18. Ramachandran R (2018) Mitochondrial dynamics: The dynamin superfamily and execution by collusion. Sem Cell Devel Biol 76, 201–212

19. Schrepfer E, and Scorrano L (2016) Mitofusins, from Mitochondria to Metabolism. Mol Cell 61, 683–694 [PubMed: 26942673]

20. Chen H, Detmer SA, Ewald AJ, Griffin EE, Fraser SE, and Chan DC (2003) Mitofusins Mfn1 and Mfn2 coordinately regulate mitochondrial fusion and are essential for embryonic development. J Cell Biol 160, 189–200 [PubMed: 12527753]

21. Chen L, Liu T, Tran A, Lu X, Tomilov AA, Davies V, Cortopassi G, Chiamvimonvat N, Bers DM, Votruba M, and Knowlton AA (2012) OPA1 mutation and late-onset cardiomyopathy: mitochondrial dysfunction and mtDNA instability. J Am Heart Assoc 1

22. Ferguson S, Raimondi A, Paradise S, Shen H, Mesaki K, Ferguson A, Destaing O, Ko G, Takasaki J, Cremona O, O' Toole E, and De Camilli P (2009) Coordinated Actions of Actin and BAR Proteins Upstream of Dynamin at Endocytic Clathrin-Coated Pits. Devel Cell 17, 811–822 [PubMed: 20059951]

23. Wakabayashi J, Zhang Z, Wakabayashi N, Tamura Y, Fukaya M, Kensler TW, Iijima M, and Sesaki H (2009) The dynamin-related GTPase Drp1 is required for embryonic and brain development in mice. J Cell Biol 186, 805–816 [PubMed: 19752021]

24. Ferguson SM, Brasnjo G, Hayashi M, Wolfel M, Collesi C, Giovedi S, Raimondi A, Gong LW, Ariel P, Paradise S, O'Toole E, Flavell R, Cremona O, Miesenbock G, Ryan TA, and De Camilli P (2007) A selective activity-dependent requirement for dynamin 1 in synaptic vesicle endocytosis. Science 316, 570–574 [PubMed: 17463283]

25. Otera H, Wang C, Cleland MM, Setoguchi K, Yokota S, Youle RJ, and Mihara KJ (2010) Mff is an essential factor for mitochondrial recruitment of Drp1 during mitochondrial fission in mammalian cells. J Cell Biol 91, 1141–1158

26. Ong S-B, Kalkhoran SB, Cabrera-Fuentes HA, and Hausenloy DJ (2015) Mitochondrial fusion and fission proteins as novel therapeutic targets for treating cardiovascular disease. Eur J Pharmacol 763, 104–114 [PubMed: 25987420]

27. Hall A, Burke N, Dongworth R, and Hausenloy D (2014) Mitochondrial fusion and fission proteins: novel therapeutic targets for combating cardiovascular disease. Br J Pharmacol 171, 1890–1906 [PubMed: 24328763]

Author Manuscript

Author Manuscript

Author Manuscript

Author Manuscript

28. Marsboom G, Toth PT, Ryan JJ, Hong Z, Wu X, Fang Y-H, Thenappan T, Piao L, Zhang HJ, and Pogoriler J (2012) Dynamin-related protein 1 (DRP1)-mediated mitochondrial mitotic fission permits hyperproliferation of vascular smooth muscle cells and offers a novel therapeutic target in pulmonary hypertension. Circ Res 110, 1484 [PubMed: 22511751]

29. Sharp WW, Fang YH, Han M, Zhang HJ, Hong Z, Banathy A, Morrow E, Ryan JJ, and Archer SL (2014) Dynamin-related protein 1 (Drp1)-mediated diastolic dysfunction in myocardial ischemia-reperfusion injury: therapeutic benefits of Drp1 inhibition to reduce mitochondrial fission. FASEB J 28, 316–326 [PubMed: 24076965]

30. Nakamura T, and Lipton SA (2016) Protein S-nitrosylation as a therapeutic target for neurodegenerative diseases. Trend Pharmacol Sci 37, 73–84

31. Zhou J, Li G, Zheng Y, Shen H-M, Hu X, Ming Q-L, Huang C, Li P, and Gao N (2015) A novel autophagy/mitophagy inhibitor liensinine sensitizes breast cancer cells to chemotherapy through DNM1L-mediated mitochondrial fission. Autophagy 11, 1259–1279 [PubMed: 26114658]

32. Fukushima NH, Brisch E, Keegan BR, Bleazard W, and Shaw JM (2001) The GTPase effector domain sequence of the Dnm1p GTPase regulates self-assembly and controls a rate-limiting step in mitochondrial fission. Mol Biol Cell 12, 2756–2766 [PubMed: 11553714]

33. Yoon Y, Krueger EW, Oswald BJ, McNiven MA (2003) The mitochondrial protein hFis1 regulates mitochondrial fission in mammalian cells through an interaction with the dynamin-like protein DLP1. Am Soc Microbiol 23, 5409–5420

34. Gandre-Babbe S, and van der Bliek AM (2008) The novel tail-anchored membrane protein Mff controls mitochondrial and peroxisomal fission in mammalian cells. Am Soc Cell Biol 19, 2402–2412

35. Palmer CS, Osellame LD, Laine D, Koutsopoulos OS, Frazier AE, and Ryan MT (2011) MiD49 and MiD51, new components of the mitochondrial fission machinery. EMBO Rep 12, 565–573 [PubMed: 21508961]

36. Zaja I, Bai X, Liu Y, Kikuchi C, Dosenovic S, Yan Y, Canfield SG, Bosnjak ZJ (2014) Cdk1, PKCδ and calcineurin-mediated Drp1 pathway contributes to mitochondrial fission-induced cardiomyocyte death. Biochem Biophysic Res Comm 453, 710–721

37. Taguchi N, Ishihara N, Jofuku A, Oka T, and Mihara KJ (2007) Mitotic phosphorylation of dynamin-related GTPase Drp1 participates in mitochondrial fission. J Biol Chem 282, 11521–11529

38. Wu Q, Luo C-L, Tao L-Y (2017) Dynamin-related protein 1 (Drp1) mediating mitophagy contributes to the pathophysiology of nervous system diseases and brain injury. J Histol Histopathol.32, 551–559

39. Nakamura T, Cieplak P, Cho D-H, Godzik A, and Lipton SA (2010) S-nitrosylation of Drp1 links excessive mitochondrial fission to neuronal injury in neurodegeneration. Mitochondrion 10, 573–578 [PubMed: 20447471]

40. Chang C-R, and Blackstone C (2007) Cyclic AMP-dependent protein kinase phosphorylation of Drp1 regulates its GTPase activity and mitochondrial morphology. J Biol Chem 282, 21583–21587 [PubMed: 17553808]

41. Chang CR, and Blackstone C (2007) Drp1 phosphorylation and mitochondrial regulation. EMBO Rep 8, 1088–1089

42. Mao D, Hou X, Talbott H, Cushman R, Cupp A, and Davis JS (2013) ATF3 expression in the corpus luteum: possible role in luteal regression. Mol Endocrinol 27, 2066–2079 [PubMed: 24196350]

43. Roy L, McDonald CA, Jiang C, Maroni D, Zeleznik AJ, Wyatt TA, Hou X, and Davis JS (2009) Convergence of 3′, 5′-cyclic adenosine 5′-monophosphate/protein kinase A and glycogen synthase kinase-3β/β-catenin signaling in corpus luteum progesterone synthesis. Endocrinology 150, 5036–5045 [PubMed: 19819952]

44. Li D, Yin X, Zmuda EJ, Wolford CC, Dong X, White MF, and Hai T (2008) The repression of IRS2 gene by ATF3, a stress-inducible gene, contributes to pancreatic β-cell apoptosis. Diabetes 57, 635–644 [PubMed: 18057093]

45. Taurin S, Sandbo N, Yau DM, Sethakorn N, and Dulin NO (2008) Phosphorylation of β-catenin by PKA promotes ATP-induced proliferation of vascular smooth muscle cells. Am J Cell Physiol 294, C1169-C1174

46. Plewes M, Burns P, Graham P, Bruemmer J, Engle T, and Barisas B (2017) Effect of fish meal supplementation on spatial distribution of lipid microdomains and on the lateral mobility of membrane-bound prostaglandin F2α receptors in bovine corpora lutea. Dom Anim Endocrinol 60, 9–18

47. Plewes M, Burns P, Graham P, Hyslop R, and Barisas B (2017) Effect of fish oil on lateral mobility of prostaglandin F2α (FP) receptors and spatial distribution of lipid microdomains in bovine luteal cell plasma membrane in vitro. Dom Anim Endocrinol 58, 39–52

48. Plewes M, and Burns P (2018) Effect of fish oil on agonist-induced receptor internalization of the PG F2α receptor and cell signaling in bovine luteal cells in vitro. Dom Anim Endocrinol 63, 38–47

49. Chang CR, and Blackstone C (2010) Dynamic regulation of mitochondrial fission through modification of the dynamin-related protein Drp1. An New York Acad Sci 1201, 34–39

50. Chen D, Fong HW, and Davis JS (2001) Induction of c-fos and c-jun messenger ribonucleic acid expression by prostaglandin F2α is mediated by a protein kinase C-dependent extracellular signal-regulated kinase mitogen-activated protein kinase pathway in bovine luteal cells. Endocrinology 142, 887–895 [PubMed: 11159862]

51. Kashatus JA, Nascimento A, Myers LJ, Sher A, Byrne FL, Hoehn KL, Counter CM, and Kashatus DF (2015) Erk2 phosphorylation of Drp1 promotes mitochondrial fission and MAPK-driven tumor growth. Mol Cell 57, 537–551 [PubMed: 25658205]

52. Chen DB, Westfall SD, Fong HW, Roberson MS, and Davis JS (1998) Prostaglandin F2alpha stimulates the Raf/MEK1/mitogen-activated protein kinase signaling cascade in bovine luteal cells. Endocrinology 139, 3876–3885 [PubMed: 9724043]

53. Pennanen C, Parra V, López-Crisosto C, Morales PE, del Campo A, Gutierrez T, Rivera-Mejías P, Kuzmicic J, Chiong M, and Zorzano A (2014) Mitochondrial fission is required for cardiomyocyte hypertrophy mediated by a Ca2+-calcineurin signaling pathway. J Cell Sci 127, 2659–2671 [PubMed: 24777478]

54. Cassidy-Stone A, Chipuk JE, Ingerman E, Song C, Yoo C, Kuwana T, Kurth MJ, Shaw JT, Hinshaw JE, and Green D. R. J. D. c. (2008) Chemical inhibition of the mitochondrial division dynamin reveals its role in Bax/Bak-dependent mitochondrial outer membrane permeabilization. 14, 193–204

55. Bertoldo MJ, Faure M, Dupont J, and Froment PJ (2014) Impact of metformin on reproductive tissues: an overview from gametogenesis to gestation. Ann Transl Med 2

56. Park J-E, Kim Y-J, Lee SG, Kim JY, Chung J-Y, Jeong S-Y, Koh H, Yun J, Park HT, and Yoo Y (2019) Drp1 phosphorylation is indispensable for steroidogenesis in Leydig cells. J Endocrinol 160, 729–743

57. Macia E, Ehrlich M, Massol R, Boucrot E, Brunner C, and Kirchhausen T (2006) Dynasore, a cell-permeable inhibitor of dynamin. Devel Cell 10, 839–850 [PubMed: 16740485]

58. Preta G, Cronin JG, Sheldon IM (2015) Dynasore-not just a dynamin inhibitor. J Cell Comm Signaling.13, 24

59. Girard E, Paul JL, Fournier N, Beaune P, Johannes L, Lamaze C, and Védie B (2011) The dynamin chemical inhibitor dynasore impairs cholesterol trafficking and sterol-sensitive genes transcription in human HeLa cells and macrophages. PLOS 6, e29042

60. Okamoto K, and Shaw JM (2005) Mitochondrial morphology and dynamics in yeast and multicellular eukaryotes. Annu Rev Genet. 39, 503–536 [PubMed: 16285870]

61. Ingerman E, Perkins EM, Marino M, Mears JA, McCaffery JM, Hinshaw JE, and Nunnari J (2005) Dnm1 forms spirals that are structurally tailored to fit mitochondria. J Cell Biol 170, 1021–1027 [PubMed: 16186251]

62. Law NC, and Hunzicker-Dunn ME (2016) Insulin Receptor Substrate 1, the Hub Linking Follicle-stimulating Hormone to Phosphatidylinositol 3-Kinase Activation. J Biol Chem 291, 4547–4560 [PubMed: 26702053]

63. Flynn MP, Fiedler SE, Karlsson AB, Carr DW, Maizels ET, and Hunzicker-Dunn M (2016) Dephosphorylation of MAP2D enhances its binding to vimentin in preovulatory ovarian granulosa cells. J Cell Sci 129, 2983–2996 [PubMed: 27335427]

64. Toyama EQ, Herzig S, Courchet J, Lewis TL, Losón OC, Hellberg K, Young NP, Chen H, Polleux F, and Chan DC (2016) AMP-activated protein kinase mediates mitochondrial fission in response to energy stress. Science 351, 275–281 [PubMed: 26816379]

65. Hou X, Arvisais EW, and Davis JS (2010) Luteinizing hormone stimulates mammalian target of rapamycin signaling in bovine luteal cells via pathways independent of AKT and mitogen-activated protein kinase: modulation of glycogen synthase kinase 3 and AMP-activated protein kinase. Endocrinology 151, 2846–2857 [PubMed: 20351317]

66. Bordt EA, Clerc P, Roelofs BA, Saladino AJ, Tretter L, Adam-Vizi V, Cherok E, Khalil A, Yadava N, and Shealinna XG (2017) The putative Drp1 inhibitor mdivi-1 is a reversible mitochondrial complex I inhibitor that modulates reactive oxygen species. Devel Cell 40, 583–594. e586 [PubMed: 28350990]

67. Otera H, and Mihara K (2012) Mitochondrial dynamics: functional link with apoptosis. Intern J Cell Biol 2012

68. Lee DG, Park J, Lee H-S, Lee S-R, and Lee D-S (2016) Iron overload-induced calcium signals modulate mitochondrial fragmentation in HT-22 hippocampal neuron cells. Toxicology 365, 17–24 [PubMed: 27481217]

69. Park J, Lee DG, Kim B, Park S-J, Kim J-H, Lee S-R, Chang K-T, Lee H-S, and Lee D-S (2015) Iron overload triggers mitochondrial fragmentation via calcineurin-sensitive signals in HT-22 hippocampal neuron cells. Toxicology 337, 39–46 [PubMed: 26318285]

70. Xiao L, Xian H, Lee KY, Xiao B, Wang H, Yu F, Shen H-M, and Liou Y-C (2015) Death-associated protein 3 regulates mitochondrial-encoded protein synthesis and mitochondrial dynamics. J Biol Chem 290, 24961–24974

71. Davis JS, Weakland LL, Weiland DA, Farese RV, and West LA (1987) Prostaglandin F2 alpha stimulates phosphatidylinositol 4,5-bisphosphate hydrolysis and mobilizes intracellular Ca2+ in bovine luteal cells. Proc Natl Acad Sci U S A 84, 3728–3732 [PubMed: 3035550]

72. Porras A, Zuluaga S, Black E, Valladares A, Alvarez AM, Ambrosino C, Benito M, and Nebreda AR (2004) p38α mitogen-activated protein kinase sensitizes cells to apoptosis induced by different stimuli. Mol Biol Cell 15, 922–933 [PubMed: 14617800]

73. Sarkar D, Su Z-Z, Lebedeva IV, Sauane M, Gopalkrishnan RV, Valerie K, Dent P, and Fisher PB (2002) mda-7 (IL-24) Mediates selective apoptosis in human melanoma cells by inducing the coordinated overexpression of the GADD family of genes by means of p38 MAPK. Proceedings of the Nat Acad Sci 99, 10054–10059

74. Tanaka Y, Gavrielides MV, Mitsuuchi Y, Fujii T, and Kazanietz MG (2003) Protein kinase C promotes apoptosis in LNCaP prostate cancer cells through activation of p38 MAPK and inhibition of the Akt survival pathway. J Biol Chem 278, 33753–33762

75. Bowdridge EC, Goravanahally MP, Inskeep EK, and Flores JA (2015) Activation of adenosine monophosphate-activated protein kinase is an additional mechanism that participates in mediating inhibitory actions of prostaglandin F2Alpha in mature, but not developing, bovine corpora lutea. Biol Reprod 93, 7, 1–7

76. Bhatt MP, Lim Y-C, Kim Y-M, and Ha K-S (2013) C-peptide activates AMPKα and prevents ROS-mediated mitochondrial fission and endothelial apoptosis in diabetes. Diabetes 62, 3851–3862 [PubMed: 23884890]

77. Li J, Wang Y, Wang Y, Wen X, Ma X-N, Chen W, Huang F, Kou J, Qi L-W, and Liu B (2015) Pharmacological activation of AMPK prevents Drp1-mediated mitochondrial fission and alleviates endoplasmic reticulum stress-associated endothelial dysfunction. J Mol Cell Cardiol 86, 62–74 [PubMed: 26196303]

78. Wikstrom JD, Israeli T, Bachar-Wikstrom E, Swisa A, Ariav Y, Waiss M, Kaganovich D, Dor Y, Cerasi E, and Leibowitz G (2013) AMPK regulates ER morphology and function in stressed pancreatic β-cells via phosphorylation of DRP1. Mol Endocrinol 27, 1706–1723 [PubMed: 23979843]

79. Morigi M, Perico L, Rota C, Longaretti L, Conti S, Rottoli D, Novelli R, Remuzzi G, and Benigni A (2015) Sirtuin 3–dependent mitochondrial dynamic improvements protect against acute kidney injury. J Clinical Invest 125, 715–726 [PubMed: 25607838]

80. Wang Q, Wu S, Zhu H, Ding Y, Dai X, Ouyang C, Han Y. m., Xie Z, and Zou M-H (2017) Deletion of PRKAA triggers mitochondrial fission by inhibiting the autophagy-dependent degradation of DNM1L. Autophagy 13, 404–422 [PubMed: 28085543]
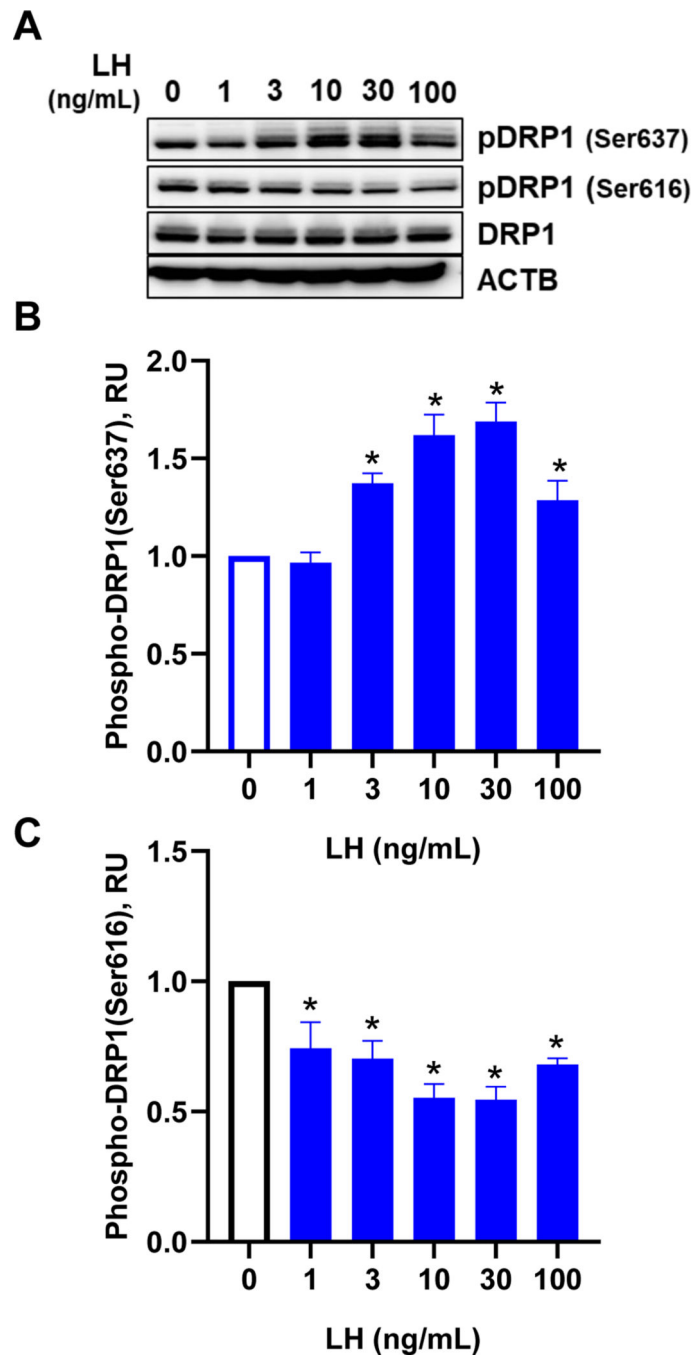
A

B

C

Figure 1. Effects of increasing concentrations of luteinizing hormone (LH) on phosphorylation of Dynamin-related protein-1 (DRP1).

Enriched cultures of small luteal cells were treated for 30 min with increasing concentrations of luteinizing hormone (LH; 0–100 ng/mL) to determine the influence of LH on stimulation of Dynamin-related protein-1 (DRP1). **Panel A:** Representative western blot analysis for phospho- and total-DRP1 proteins. **Panel B:** Densitometric analyses of phospho-DRP1 (Ser637). **Panel C** Densitometric analyses of phospho-DRP1 (Ser616). Bars represent

means ± sem, n = 3. [**]Significant difference between treatments as compared to Control, $P < 0.05$.
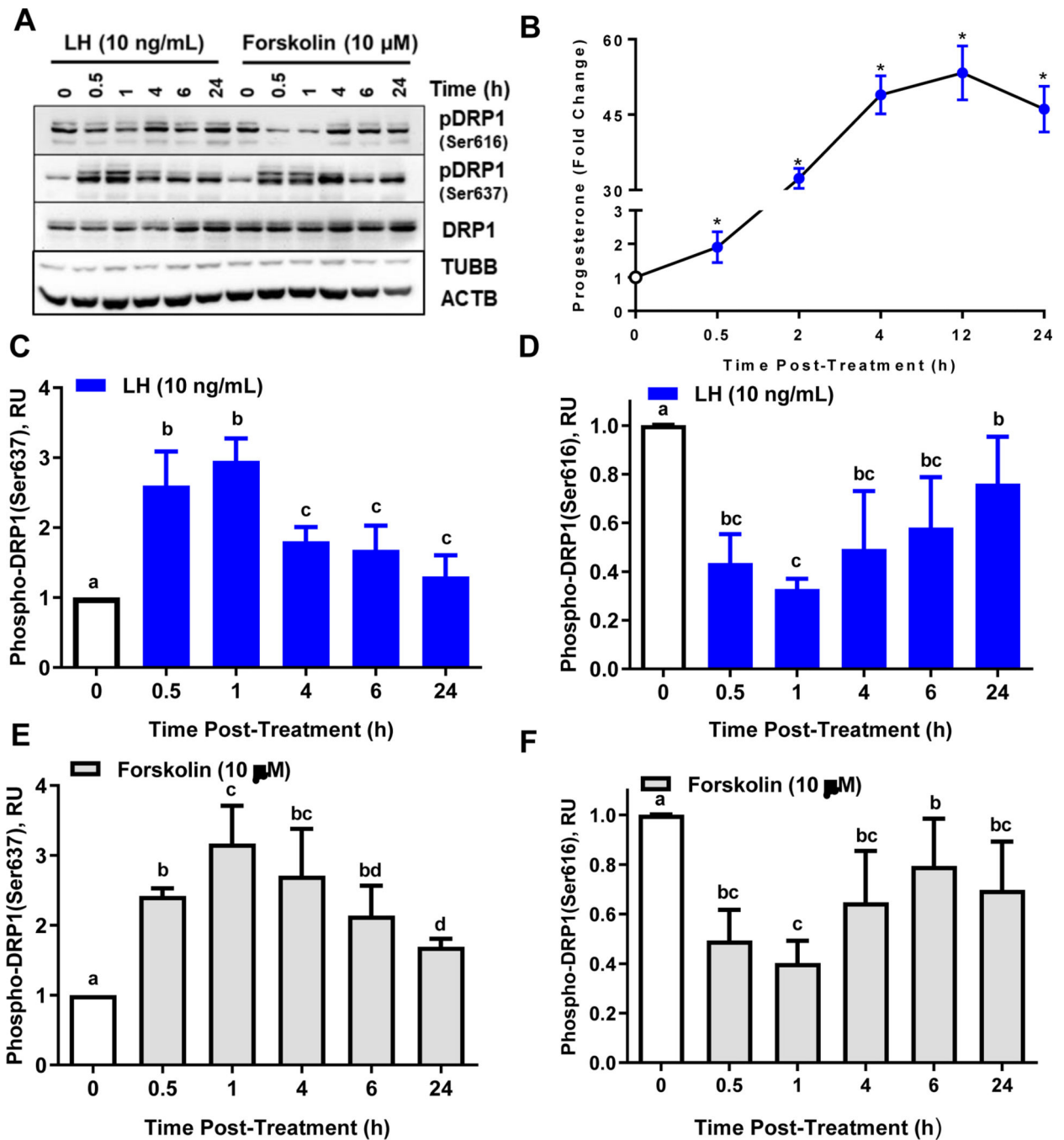
Figure 2: Temporal effects of luteinizing hormone (LH) or forskolin on phosphorylation of Dynamin-related protein-1 (DRP1).

Small bovine luteal cells were treated with LH (10 ng/mL) or forskolin (10 μM) for 0, 0.5, 1, 4, 6, or 24 h. Protein was extracted and subject to western blotting. Progesterone in the culture medium was measured by ELISA. **Panel A:** Representative western blot analysis on phosphorylation of DRP1 in small luteal cells. **Panel B:** Fold increase in progesterone following treatment with LH. *Significantly different from control, $P < 0.05$. **Panel C:** Densitometric analyses of phospho-DRP1 (Ser637). **Panel D:** Densitometric analyses of

phospho-DRP1 (Ser616). **Panel E:** Densitometric analyses of phospho-DRP1 (Ser637). **Panel F:** Densitometric analyses of phospho-DRP1 (Ser616). **Panels C-F:** Bars represent mean fold changes (means ± sem, n = 3). Open bars: Control 0-h. Closed bars: LH or forskolin-treated cells. Bars with different letters[abcd] differ significantly within treatment (P < 0.05).
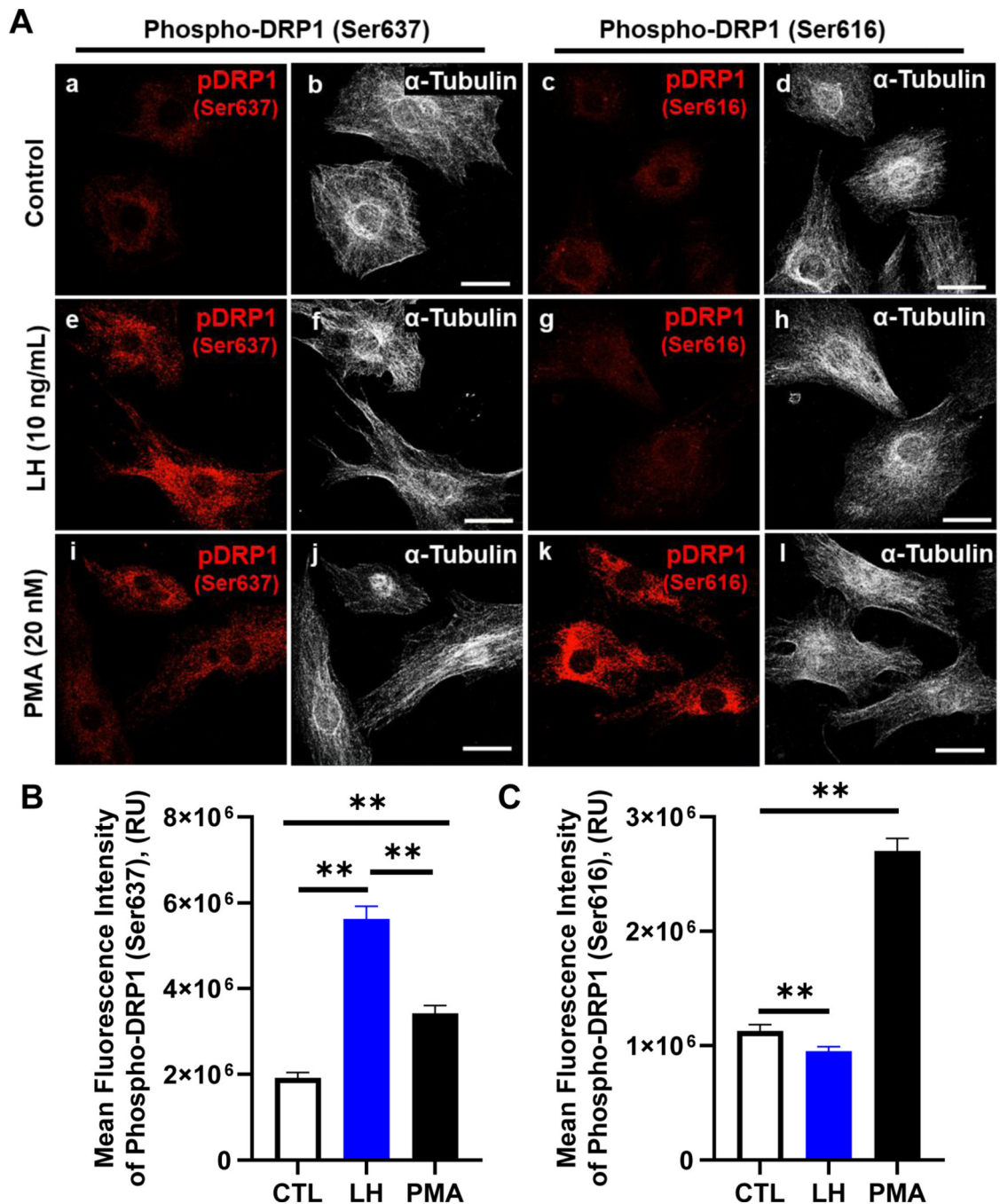
Figure 3: Effects of luteinizing hormone (LH) or Phorbol 12-myristate 13-acetate (PMA) on the phosphorylation of Dynamin-related protein-1 (DRP1).
Bovine small luteal cells were treated with vehicle control (CTL), luteinizing hormone (LH; 10 ng/mL) or the PKC activator, Phorbol 12-myristate 13-acetate (PMA; 20 nM) for 30 min and subject to confocal microscopy. **Panel A:** Representative micrographs showing the effects of Control, LH or PMA on phosphorylation of DRP1 Ser 637 and Ser616 in small luteal cells. Control (a-d), LH (e-h), and PMA (i-l). **Panel B:** Quantitative analyses of the mean fluorescence intensity of phospho-DRP1 (Ser637). **Panel C:** Quantitative analyses of

the mean fluorescence intensity of phospho-DRP1 (Ser616). Bars represent means ± sem (n = 3). Open bars represent control cells (0-h); Closed blue bars represent LH-treated cells; Closed black bars represent PMA-treated cells. [**]Significant difference between treatments as compared to Control, $P < 0.05$.
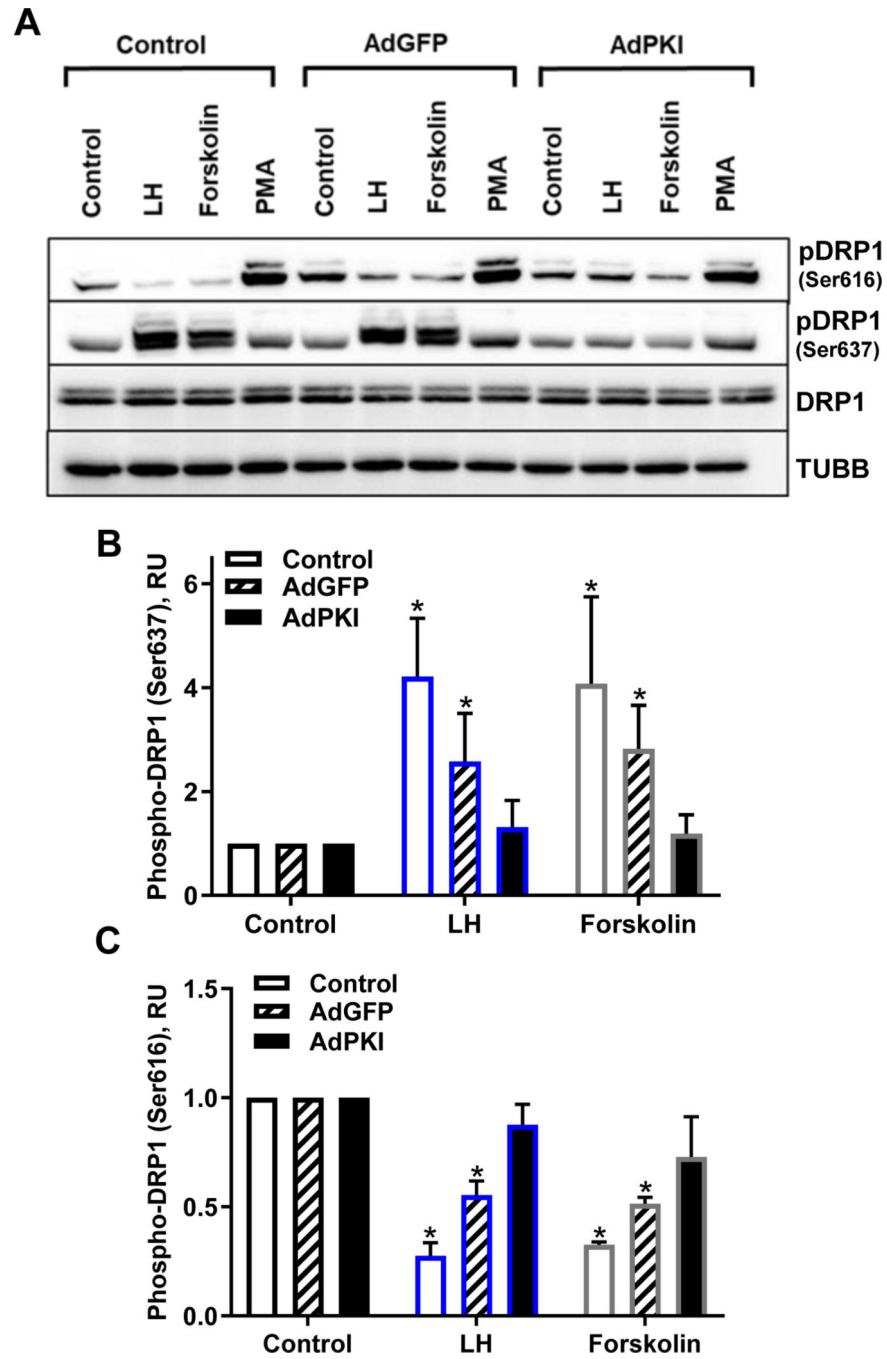
Figure 4: Effects of overexpression of Protein Kinase Inhibitor peptide (PKI) on phosphorylation of Dynamin-related protein-1 (DRP1).

Bovine small luteal cells were treated with replication-deficient adenoviruses containing the complete sequence of endogenous green fluorescent protein (GFP) (Ad.GFP) or Protein Kinase Inhibitor (PKI) (*Ad.PKI*) to overexpress GFP or PKI. Following infection, cells were treated with vehicle control, luteinizing hormone (LH; 10 ng/mL), forskolin (10 μM), or phorbol 12-myristate 13-acetate (PMA; 20 nM). Succeeding treatment, protein was extracted and subject to western blotting. **Panel A:** Representative western blot analysis of the

phosphorylation of DRP1. **Panel B:** Densitometric analyses of phospho-DRP1 (Ser637). **Panel C:** Densitometric analyses of phospho-DRP1 (Ser616). Bars represent means ± sem, n = 3. *Significant difference between treatments as compared to Control, *P* < 0.05.
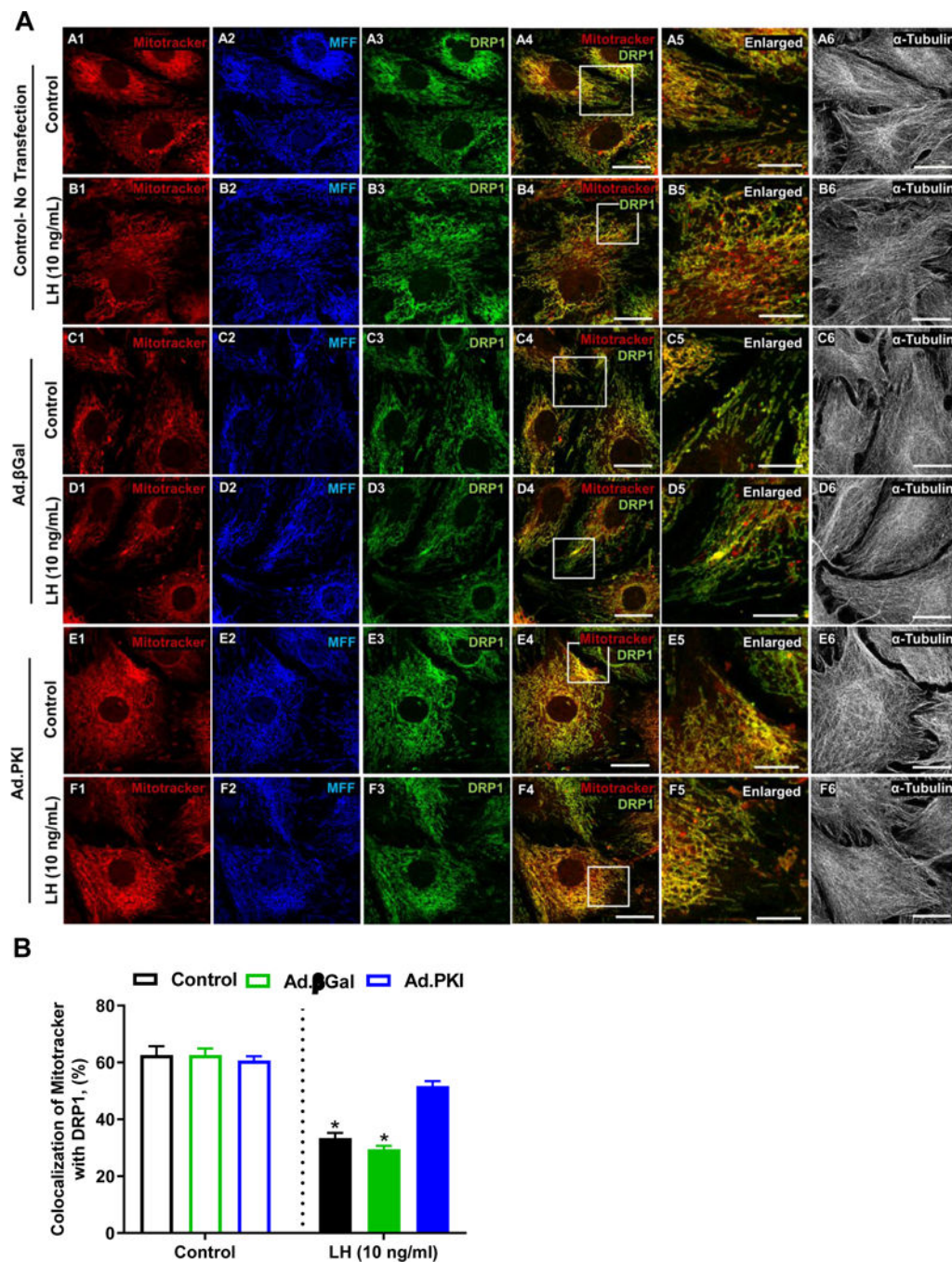
Figure 5: Luteinizing hormone (LH) inhibits colocalization of Dynamin-related protein-1 (DRP1) on mitochondria.

Replication-deficient adenoviruses containing the complete sequence of endogenous β-galactosidase (Ad.βGal) and Protein Kinase Inhibitor (PKI) (*Ad.PKI*) were utilized to overexpress βGal or PKI in small bovine luteal cells. Following infection, cells were treated with luteinizing hormone (LH; 10 ng/mL) for 4 h. Succeeding treatment, confocal microscopy was used to determine the influence of LH on colocalization of DRP1 with mitochondria. **Panel A:** Representative micrographs of (left to right) Mitotracker (A-F1),

MFF (A-F2), DRP1 (A-F3), merge of Mitotracker and DRP1 (A-F4), enlarged inlet of colocalization (A-F5), and alpha-Tubulin (A-F6) and (top to bottom) No Transfection SLC control (A#), No Transfection SLC + LH (B#), Ad.βGal viral control (C#), Ad.βGal viral control + LH (D#), Ad.PKI (E#), Ad.PKI + LH (F#). The micron bar represents 10 and 20 μm. **Panel B:** Quantitative analysis of the colocalization of Mitotracker with DRP1. Bars represent means ± standard error. *Significant difference between treatment, $P < 0.05$.
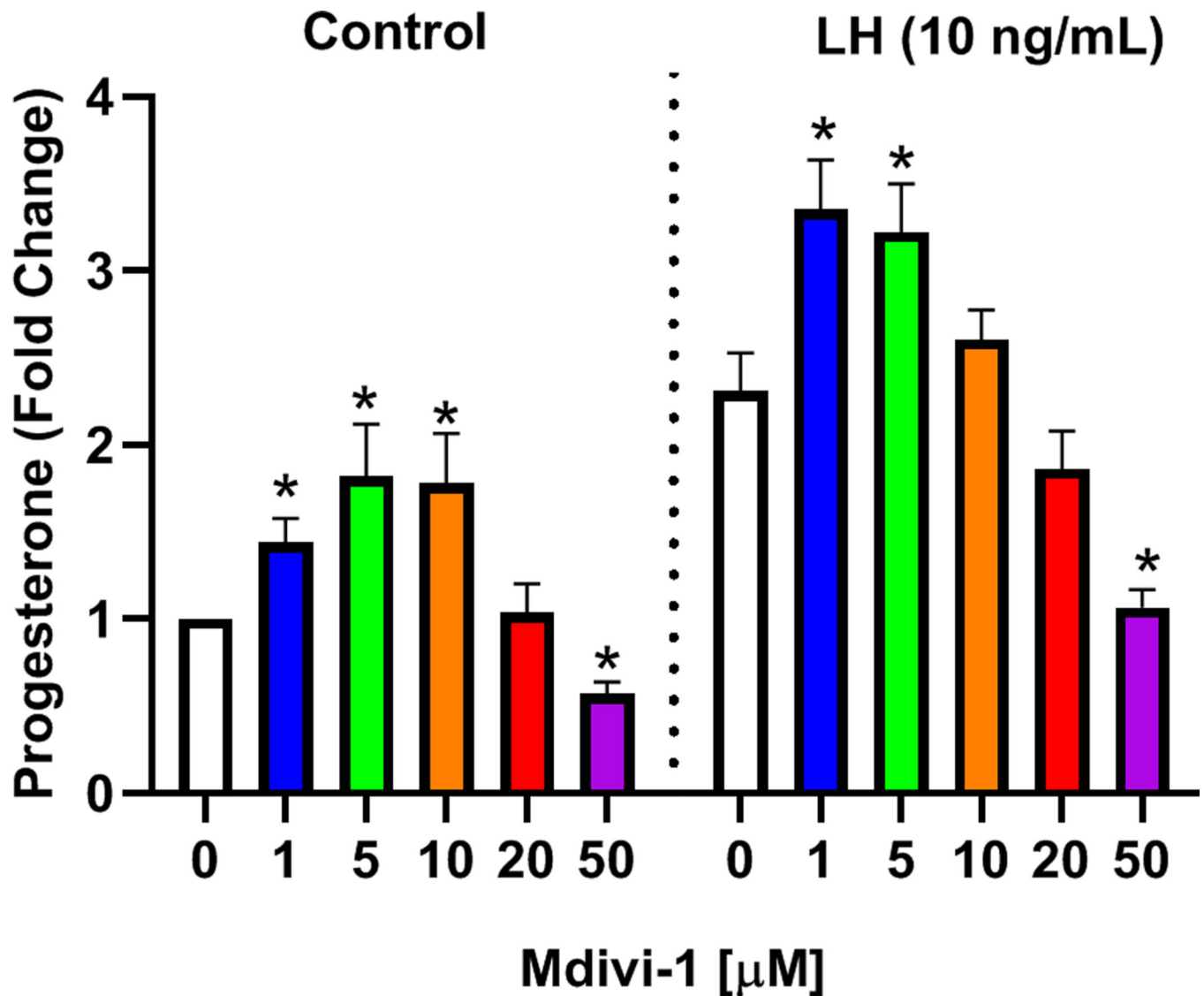
Figure 6: Effects of Selective Dynamin related protein 1 (DRP1) inhibitor, Mdivi-1, on basal and luteinizing hormone (LH)-induced progesterone production.
Small bovine luteal cells were pretreated with increasing concentrations of the cell-permeable DRP1 inhibitor Mdivi-1 (0 – 50 μM) for 2 h and subsequently treated with 10 ng/mL luteinizing hormone (LH) for 4-h. Following treatment progesterone was quantified by ELISA. Bars represent means ± standard error, n = 4 experiments. *Significant difference as compared to respective controls, $P < 0.05$.
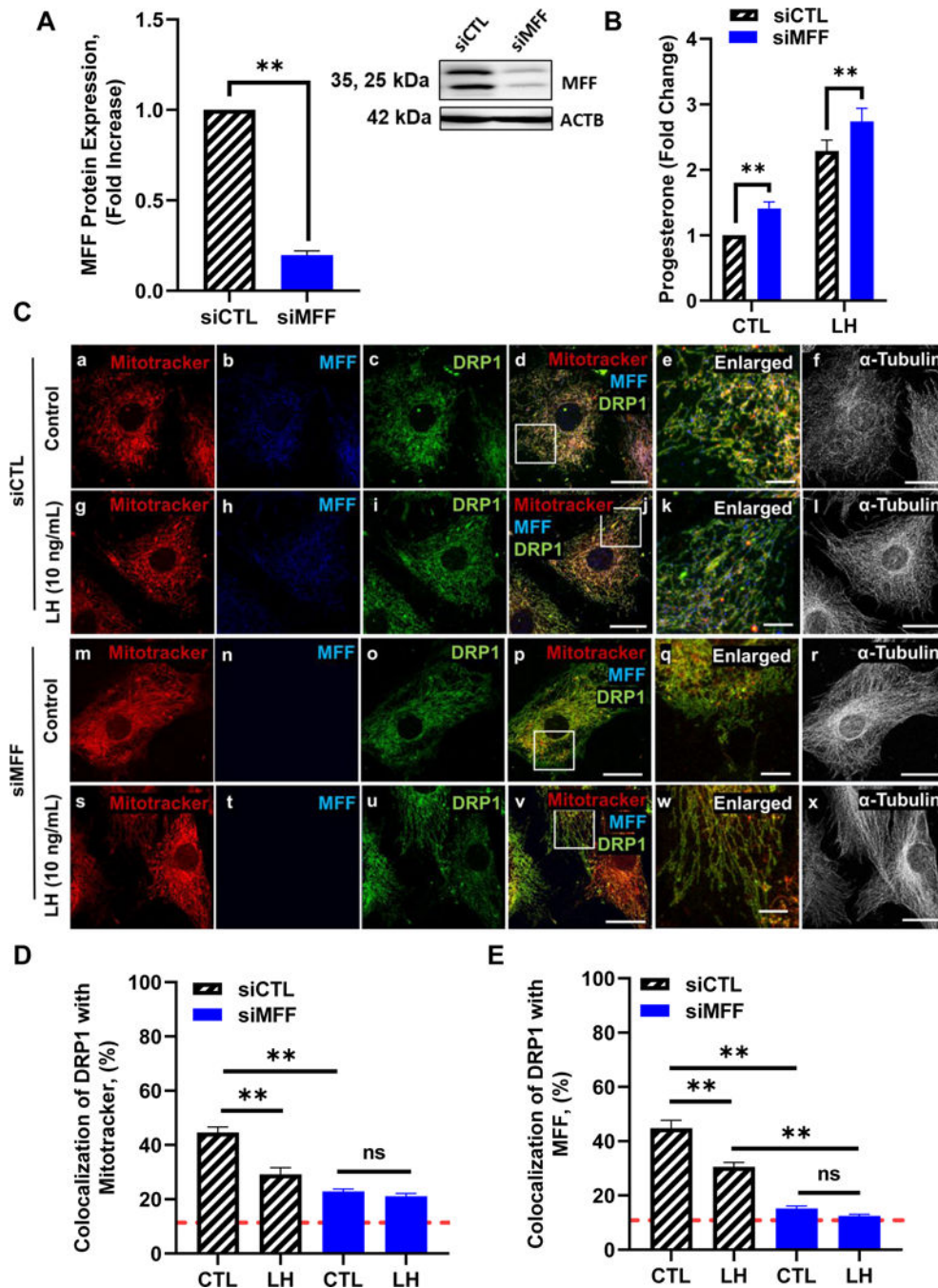
Figure 7: Effects of knockdown of mitochondrial fission factor (MFF) on progesterone production and DRP1 localization in bovine small luteal cells.

Mitochondrial fission factor (MFF) mRNA was silenced using siMFF in small bovine luteal cells. Following knockdown, cells were treated without (Control) or with luteinizing hormone (LH; 10 ng/mL) for 4 h. **Panel A:** Densitometric analyses of MFF protein expression. Bars represent means ± sem, n = 4. Inset representative western blot analysis showing expression of MFF in siMFF knockdown small luteal cells. **Panel B:** Medium progesterone. Bars represent means ± sem, n = 6. *Significant difference between treatment

as compared to control, $P < 0.05$. **Significant difference within treatment (CTL or LH), $P < 0.05$. **Panel C:** Representative micrographs of (left to right) Mitotracker (a, g, m and s), MFF (b, h, n and t), DRP1 (c, i, o and u), merge of Mitotracker, MFF, and DRP1 (d, j, p and v), enlarged inlet of colocalization (e, k, q and w), and alpha-Tubulin (f, l, r and x) and (top to bottom) siCTL (a-f), siCTL + LH (10 ng/mL; g-l), siMFF (m-r) and siMFF + LH (10 ng/mL; s-x), enlarged image (white box corresponding to adjacent image). **Panel D:** Quantitative analysis of the colocalization of DRP1 with Mitotracker. **Panel E:** Quantitative analysis of the colocalization of DRP1 with MFF. Bars represent means ± standard error; n = 3. Red dashed line indicated analysis cut-off set at 10% colocalization. **Significant difference between treatment (control vs LH), $P < 0.05$.
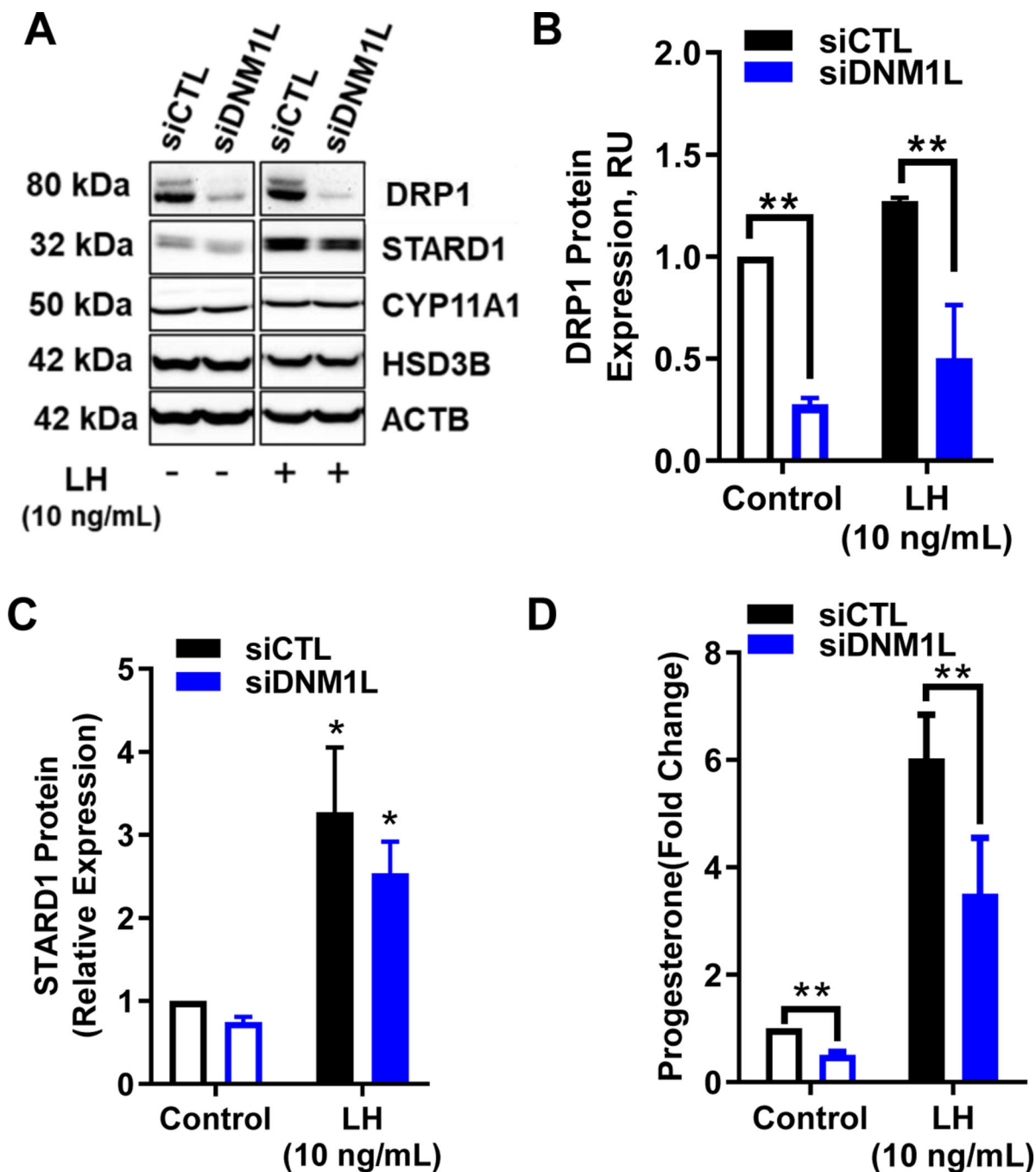
Figure 8: Effects of knockdown of Dynamin-related protein-1 (DRP1) on steroidogenic protein expression and progesterone production in small bovine luteal cells.
Dynamin-related protein-1 (DRP1) mRNA was silenced using siDNM1L in small bovine luteal cells. Following knockdown, cells were treated without (Control) or with luteinizing hormone (LH; 10 ng/mL) for 4 h. **Panel A:** Representative western blot analysis showing expression of DRP1 and steroidogenic proteins. **Panel B:** Densitometric analyses of DRP1 protein expression. Bars represent means ± sem, n = 5. **Panel C:** Densitometric analyses of STAR protein expression. Bars represent means ± sem, n = 3. **Panel D:** Medium

progesterone. Bars represent means ± sem, n = 3. *Significant difference between treatment as compared to control, $P < 0.05$. **Significant difference within treatment, $P < 0.05$.

Table 1:

Characteristics of antibodies used for western blotting and microscopy

Antibody name	Dilution ratio	Species specificity	Source	Supplier (distributor, town, country)	Cat. No
Phospho-DRP1 (Ser637)	1:1000^1 / 1:200^2	Mouse	Rabbit mAB	Cell Signaling (Boston, MA, USA)	4867S
Phospho-DRP1 (Ser616)	1:1000^1 / 1:200^2	Human	Rabbit mAB	Cell Signaling	4494S
DRP1	1:1000^1/1:200^2/1:200 *	Mouse	Rabbit mAB	Cell Signaling	8570S
MFF	1:1000^1 / 1:200^2	Mouse	Rabbit pAB	Cell Signaling	86668S
STAR	1:10000	Mouse	Rabbit pAB	Abcam (Cambridge, United Kingdom)	ab96637
CYP11A1	1:1000	Mouse	Rabbit mAB	Cell Signaling	14217
HSD3B	1:1000	Mouse	Rabbit mAB	A gift from Dr. Ian Mason	
TOM20	1:200 *	Mouse	Rabbit mAB	Cell Signaling	42406S
ACTB	1:5000	Bovine	Mouse mAB	Sigma Life Science (St. Louis, Missouri, USA)	A5441
Beta-tubulin	1:5000	Bovine	Mouse mAB	Sigma Life Science	T4026
Alpha-tubulin	1:200	Bovine	Mouse mAB	Abcam	ab7291
HRP-linked	1:10000	Anti-rabbit		Jackson ImmunoResearch (West Grove, PA, USA)	111035003
HRP-linked	1:10000	Anti-mouse		Jackson Laboratory	115035205
Alexa Fluor 488	1:500	Anti-mouse		Invitrogen (Carlsbad, CA, USA)	A32723
Alexa Fluor 594	1:500	Anti-rabbit		Invitrogen	A-11032
Alexa Fluor 647	1:500	Anti-biotin		Biolegend (San Diego, CA, USA)	405237
TopFluor Cholesterol	5 μM			Avanti Lipids	810255

[1] Diltuion used for Western Blotting

[2] Diltuion used for Confocal Microscopy

* Biotinylated Antibody

Dynamin related protein 1 (DRP1); Mitochondrial fission factor (MFF); Steroidogenic acute regulatory protein (STAR); 3beta-Hydroxysteroid dehydrogenase (HSD3B); Cholesterol side-chain cleavage enzyme (CYP11A1); Mitochondrial import receptor subunit (TOM20); Beta-actin (ACTB; loading control); Beta-tubulin (TUBB; loading control); Alpha-tubulin (TUBA).